HP1α recruitment to DNA damage by p150CAF-1 promotes homologous recombination repair

Céline Baldeyron,[1,2] Gaston Soria,[1,2] Danièle Roche,[1,2] Adam J. L. Cook,[1,2] and Geneviève Almouzni[1,2]

[1]Institut Curie, Centre de Recherche, Paris, F-75248 France
[2]UMR218, Laboratory of Nuclear Dynamics and Genome Plasticity, Centre National de la Recherche Scientifique, Paris, F-75248 France

Heterochromatin protein 1 (HP1), a major component of constitutive heterochromatin, is recruited to DNA damage sites. However, the mechanism involved in this recruitment and its functional importance during DNA repair remain major unresolved issues. Here, by characterizing HP1α dynamics at laser-induced damage sites in mammalian cells, we show that the de novo accumulation of HP1α occurs within both euchromatin and heterochromatin as a rapid and transient event after DNA damage. This recruitment is strictly dependent on p150CAF-1, the largest subunit of chromatin assembly factor 1 (CAF-1), and its ability to interact with HP1α. We find that HP1α depletion severely compromises the recruitment of the DNA damage response (DDR) proteins 53BP1 and RAD51. Moreover, HP1α depletion leads to defects in homologous recombination–mediated repair and reduces cell survival after DNA damage. Collectively, our data reveal that HP1α recruitment at early stages of the DDR involves p150CAF-1 and is critical for proper DNA damage signaling and repair.

Introduction

The survival of all living organisms depends on the faithful maintenance of their genome, the integrity of which is constantly challenged by physiological processes and environmental genotoxic agents. Thus, cells have evolved an elaborate network, the DNA damage response (DDR), to counteract the potentially deleterious effects of DNA damage (Hoeijmakers, 2001; Jackson and Bartek, 2009). Eukaryotic genomic DNA is organized into chromatin, a nucleoprotein complex in which histones play a major role to form its basic unit, the nucleosome (Kornberg and Klug, 1981). Chromatin can adopt further levels of compaction involving non-histone proteins, as in the case of densely compacted heterochromatin regions. Overall, this organization can impose structural constraints that limit access of proteins involved in DNA metabolism (transcription, replication, DDR, and recombination; Groth et al., 2007b).

Much progress has been made in characterizing the modifications of chromatin during DNA repair (Polo and Almouzni, 2007; Misteli and Soutoglou, 2009), especially at the nucleosomal level (Corpet and Almouzni, 2009; van Attikum and Gasser, 2009). One of the best-characterized modifications is the phosphorylation of histone H2AX by phosphatidylinositol-3′-OH kinase-related kinases (PIKK), such as ataxia telangiectasia mutated (ATM), after the induction of DNA double strand breaks (DSBs). Phosphorylated H2AX (γH2AX) spreads rapidly over megabases on the adjacent chromatin (Rogakou et al., 1998, 1999). In turn, γH2AX serves as a platform to attract and retain proteins that are subsequently recruited, which sense or signal the presence of breaks, such as Nijmegen breakage syndrome 1 (NBS1), mediator of DNA damage checkpoint protein 1 (MDC1), breast cancer susceptibility 1 (BRCA1), or p53-binding protein 1 (53BP1), leading to the recruitment of DNA repair proteins (Kinner et al., 2008; Lisby and Rothstein, 2009). The final output is the repair of DSBs by two major pathways: nonhomologous end-joining (NHEJ) and homologous recombination (HR; van Gent et al., 2001; Wyman and Kanaar, 2006). However, beyond DNA and histones, our knowledge of how non-histone proteins influence signaling and repair of DNA damage is limited.

Correspondence to Geneviève Almouzni: genevieve.almouzni@curie.fr

C. Baldeyron's present address is Translational Research Dept., Breast Cancer Biology Group, F-75248 France.

Abbreviations used in this paper: 6,4-PP, pyrimidine 6,4-pyrimidone photoproduct; ATM, ataxia telangiectasia mutated; CPD, cyclobutane pyrimidine dimer; CtIP, C-terminal binding protein interacting protein; DDR, DNA damage response; DSB, DNA double strand break; HR, homologous recombination; IB, immunoblotting; IF, immunofluorescence; IR, ionizing radiation; MEF, mouse embryonic fibroblast; NER, nucleotide excision repair; NHEJ, nonhomologous end-joining; UTR, untranslated region; wt, wild type.

The Rockefeller University Press $30.00
J. Cell Biol. Vol. 193 No. 1 81–95
www.jcb.org/cgi/doi/10.1083/jcb.201101030

Recent studies showed that in mammalian cells, chromatin undergoes local expansion within seconds of laser microirradiation-induced DNA damage (Kruhlak et al., 2006). This phenomenon occurs in both euchromatin and heterochromatin with similar kinetics, yet each domain responds differently to DNA damaging agents. For example, after ionizing radiation (IR), the majority of γH2AX foci are located outside of or close to heterochromatin domains (Cowell et al., 2007; Kim et al., 2007), which suggests that heterochromatin limits the access of DDR proteins to DNA. This hypothesis is consistent with the fact that DSB repair takes longer to proceed in heterochromatin compared with euchromatin and specifically requires the activity of ATM (Goodarzi et al., 2008). These data have lead to the general view that heterochromatin factors should be removed or counteracted to allow relaxation of chromatin structure and facilitate DNA damage signaling and repair.

However, the prevailing model does not adequately explain the complex behavior of HP1 proteins after DNA damage that was revealed recently by different groups (Ayoub et al., 2009; Luijsterburg et al., 2009; Zarebski et al., 2009). These three groups found that all HP1 proteins (HP1α, HP1β, and HP1γ) accumulate at DNA damage sites. At heterochromatin domains, HP1 recruitment seems to occur after an initial dispersion step, at least for HP1β (Ayoub et al., 2008, 2009). These distinct dynamics of HP1 at DSBs (Ayoub et al., 2009; Dinant and Luijsterburg, 2009) underline the need to further explore the molecular determinants of HP1 targeting and the functional relevance of HP1 in DDR.

The first hint as to the determinants of HP1 recruitment to DNA lesions came from the discovery of a requirement for the chromoshadow domain (CSD) of HP1 (Luijsterburg et al., 2009). This domain is known to interact with proteins that contain a PxVxL motif, among which KAP-1, the transcriptional corepressor KRAB-associated protein 1 (Ryan et al., 1999), and p150CAF-1 (Murzina et al., 1999; Thiru et al., 2004), the largest subunit of chromatin assembly factor 1 (CAF-1), a histone H3-H4 chaperone, are of particular interest. Both KAP-1 and p150CAF-1 are in complexes with HP1 (Loyola et al., 2009), and, importantly, the interaction of p150CAF-1 with HP1 in mouse cells is critical for the duplication of pericentric heterochromatin (Quivy et al., 2004, 2008). Thus, examining KAP-1 and p150CAF-1 is particularly relevant for understanding HP1 dynamics at DNA damage sites.

In this study, we investigated HP1, p150CAF-1, and KAP-1 dynamics at DNA lesions using a system in which local DNA damage is induced by laser microirradiation. We found that all isoforms of HP1 are transiently recruited to damage sites, a result consistent with the fact that they can heterodimerize. We then focused on HP1α and found that its accumulation at DNA lesions is independent of the usual parameters required for stable HP1 accumulation at constitutive heterochromatin, such as the Suv39 histone methyltransferase, H3K9me3, and noncoding RNA, but that it requires binding to p150CAF-1. We thus uncover a novel mechanism for the transient recruitment of HP1 at DNA damage sites, which differs from the one implicated in the maintenance of its stable enrichment at constitutive heterochromatin. Notably, we observed that although the depletion of HP1α, p150CAF-1, or KAP-1 do not significantly affect H2AX phosphorylation, the recruitment of 53BP1 and the DNA repair protein RAD51 were strongly impaired. In line with this, by using powerful reporter assays we found that HP1α depletion impairs the efficiency of HR and leads to a defect during the DNA end-resection step. Therefore, the data presented herein put forward a novel important role for p150CAF-1 and HP1α in DNA damage signaling and repair that broadens our views concerning their cellular function, beyond a histone chaperone for p150CAF-1 and beyond a mere component of heterochromatin for HP1α.

Results

Dynamics of HP1 and p150CAF-1 recruitment to DNA damage in euchromatin and heterochromatin

We induced localized DNA damage by presensitization with Hoechst 33258 followed by irradiation with a 405 nm laser, an experimental setup previously exploited for studying HP1 behavior after DNA damage (Ayoub et al., 2008, 2009; Luijsterburg et al., 2009). This method proved efficient in our hands to specifically generate damage that leads specifically to recruitment of DDR proteins involved in the cellular response to DSBs (Fig. S1, A–D). Confident in our setup, we started by examining HP1 dynamics at DNA damage sites in mouse cells because their constitutive heterochromatin, highly enriched in HP1 proteins (Fig. S2 A), can be readily visualized as chromocenters, which stain densely with fluorescent DNA dyes (Maison and Almouzni, 2004). After transient expression of GFP-tagged mouse HP1α (GFP-mHP1α), we irradiated single chromocenters as a whole domain (Fig. 1 A). As described for HP1β (Ayoub et al., 2008), at early time points after laser irradiation on a single chromocenter, we observed a general spreading of the GFP-mHP1α signal. This spreading was dependent on the presence of DSBs, as it only occurred when cells were presensitized with Hoechst (Fig. 1 B, compare with Fig. S1 E in the absence of Hoechst presensitization). At the same time, Hoechst staining revealed an expansion of the chromocenter after DNA damage (Fig. 1 B, Hoechst panels). Importantly, we also examined under the same conditions the behavior of the largest subunit of CAF-1, p150CAF-1. After damaging a whole chromocenter in cells stably expressing GFP-mp150, we observed a clear accumulation of p150CAF-1 within the area of chromatin expansion, which peaked in intensity in a range of 5 min (Fig. 1 C). To examine closely the response to DNA damage within this time frame, we performed microirradiation in stripes. This experimental setting allowed us to compare heterochromatin to euchromatin regions within the same nucleus and to study chromocenters that were only partially damaged (Fig. 1 D). We followed the endogenous proteins by immunostaining after Triton X-100 extraction that removes the soluble pools. In euchromatin, both HP1α and p150CAF-1 accumulated with similar kinetics (Fig. 1 E, 5 min panel). At pericentric heterochromatin, where preexisting HP1α signal was clearly visible, the intensity of HP1α staining further increased. This was particularly evident with our method when a chromocenter was partially

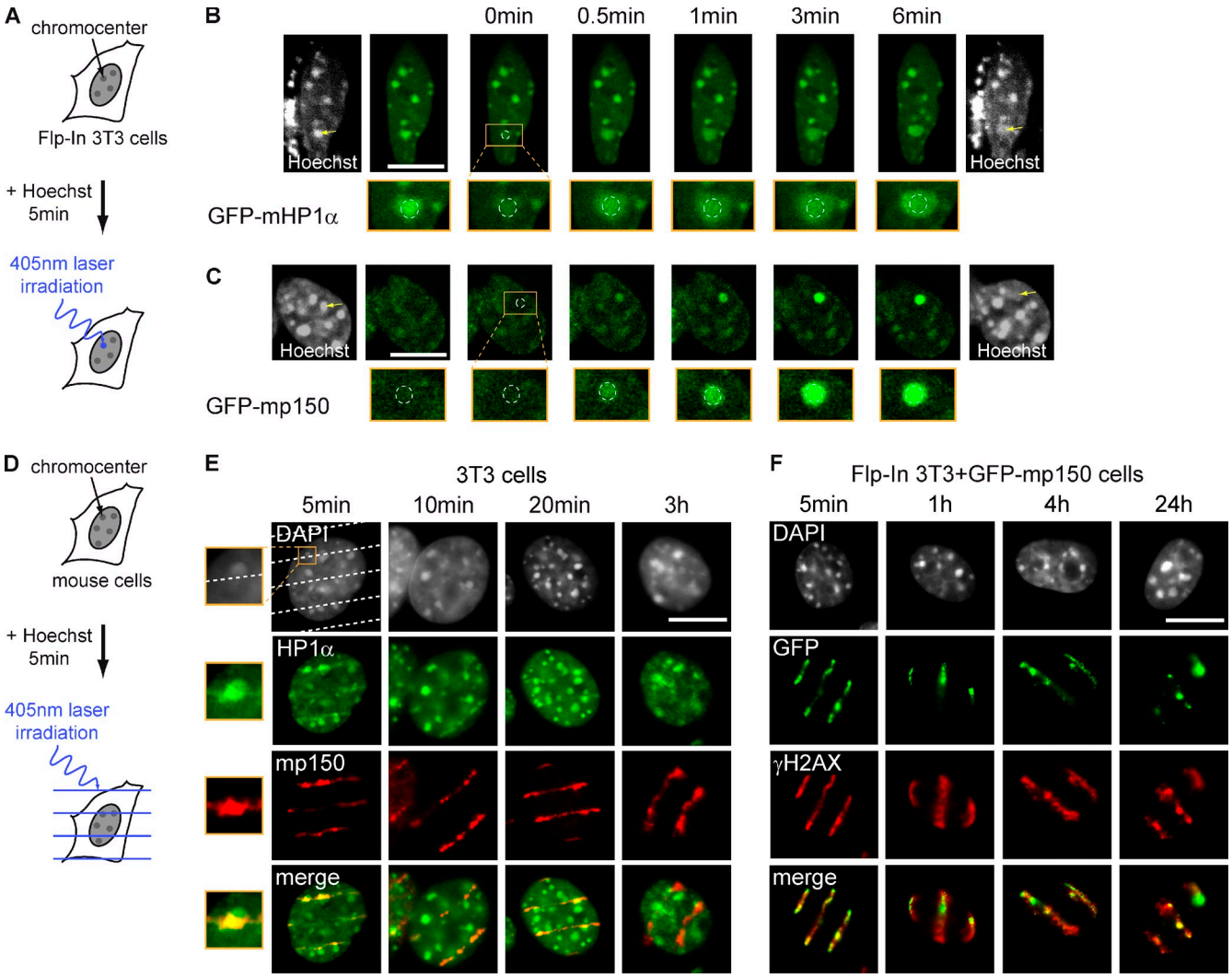

Figure 1. **HP1α and p150CAF-1 recruitment after DNA damage induction.** (A) Experimental scheme for DNA damage induction in spots. To analyze the behavior of HP1α and p150CAF-1 after DNA lesions induced in a pericentric heterochromatin domain, we selected and microirradiated with a 405 nm laser a single chromocenter (blue circle) in Hoechst presensitized cells. Immediately after, we performed live cell imaging on a confocal microscope and monitored the behavior of GFP-tagged proteins at the targeted chromocenter. (B and C) GFP-mHP1α (B) and GFP-mp150 (C) behavior after 405 nm laser irradiation. In mouse Flp-In 3T3 cells transiently transfected with pcDNA5/FRT+GFP-mHP1α plasmid (B) or Flp-In 3T3+GFP-mp150 cells (C), we irradiated a single chromocenter (white circles) as described in A. We show enlarged images of the damaged areas (orange boxes below) and Hoechst staining of live cells before damage induction and at the end of experiment. The yellow arrows on Hoechst images indicate the chromocenter that was damaged. (D) Experimental scheme for DNA damage induction in lines. We sensitized mouse cells with Hoechst for 5 min at 37°C and subsequently performed local 405 nm laser irradiation in parallel lines (blue lines). At the indicated time after DNA damage induction, we permeabilized cells with CSK + Triton X-100 to remove soluble nuclear components and fixed them for subsequent IF analyses. (E) Transient HP1α accumulation at laser-induced DNA damage sites. We treated 3T3 cells as in D and we performed coimmunostaining with anti-HP1α and anti–mouse p150CAF-1 (mp150) antibodies. We show in the 5 min panel enlarged views of a damaged area (orange boxed region) containing a chromocenter that was partially damaged and the neighboring euchromatic region. (F) Persistence of p150CAF-1 at laser-induced DNA damage sites. We treated Flp-In 3T3+GFP-mp150 cells as previously. We performed immunostaining with an anti-γH2AX antibody and visualized p150CAF-1 by the direct detection of GFP signal. DNA is stained with DAPI. Bars, 10 µm.

damaged, as HP1α staining increased only in the damaged area (Fig. 1 E, enlarged 5 min panel). Thus, although analysis of the damage-induced HP1 dynamics performed, respectively, for heterochromatin and euchromatin in distinct cells have led to the idea that both regions may behave in a different manner (Ayoub et al., 2008, 2009; Luijsterburg et al., 2009; Zarebski et al., 2009), our data show that when the analysis is performed in the same nucleus, HP1α accumulates in both chromatin subdomains in a similar time frame (Fig. 1 E). Remarkably, as for HP1α, p150CAF-1 also accumulated at laser-induced lesions with a stronger signal in the damaged part of chromocenters (Fig. 1 E, enlarged 5 min panel), along with p60CAF-1, another subunit of CAF-1 (Fig. S2 F). This recruitment of p150CAF-1 to DNA damage sites occurred in cells both inside and outside S phase, as revealed by the typical CAF-1 staining patterns across the cell cycle (Fig. S2, C–E; Quivy et al., 2004, 2008). Furthermore, the recruitment of both p150CAF-1 and HP1α at laser-induced damage sites occurred efficiently in cells deficient in nucleotide excision repair (NER; Fig. S3, A and B) and concomitantly with the recruitment of early DDR signaling proteins such as ATM, NBS1, 53BP1, BRCA1, and FANCD2 (Fig. S3 C), and repair proteins such as RAD51 and KU80 involved in HR

and NHEJ, respectively (Fig. S3 D). Thus, this novel type of p150CAF-1 recruitment observed here could not be related to the previously described role of CAF-1 in NER as a chaperone-promoting histone deposition at the end of DNA repair (Green and Almouzni, 2003; Polo et al., 2006).

Notably, HP1α accumulation rapidly disappeared, becoming almost undetectable 30 min after laser irradiation (Fig. 1 E). This behavior is similar to that observed for HP1β and HP1γ (Fig. S4 A), with which HP1α can heterodimerize, and to that observed for KAP-1 (Ziv et al., 2006), another known interacting partner of HP1. In contrast, p150CAF-1, which was recruited as early as HP1α, did not dissociate as quickly as HP1α (Fig. 1 E). Rather, it remained localized at damage sites for as long as we could detect γH2AX (Fig. 1 F). Together, these observations indicate that HP1 proteins might act transiently at damaged DNA, whereas p150CAF-1 is likely to be necessary for a longer time frame, possibly during both early and late steps of the DDR.

The recruitment of HP1α and KAP-1 to DNA damage depends on p150CAF-1

To explore the mechanism by which HP1α is recruited to damage, we first examined classical heterochromatin marks. We found that HP1α accumulated at laser-induced DNA damage sites regardless of the enrichment for H3K9me3 (Fig. S4 C), which is consistent with previous findings (Ayoub et al., 2008), and independently of Suv39 (Fig. S4 E), as found in Luijsterburg et al. (2009). Furthermore, although RNase A treatment removed HP1α from pericentric heterochromatin (Maison et al., 2002), it did not affect HP1α accumulation at DNA damage sites where p150CAF-1 got recruited (Fig. S4 D). Thus, the transient HP1α accumulation at laser-induced breaks does not rely on the typical hallmarks of stable pericentric heterochromatin and rather represents a distinct process. This prompted us to consider if this process could involve cooperation between HP1α and its known partners p150CAF-1 and KAP-1, which we also found recruited to laser-induced damage sites. To investigate this question, and to avoid the complications caused by enrichment in HP1α at chromocenters in mouse cells, we chose to use human U2OS cells in which damage-induced accumulation is easier to follow because they do not display cytologically visible heterochromatic regions (Fig. S2 B). These cells also proved convenient for efficient depletion of HP1α, KAP-1, and p150CAF-1 proteins using siRNAs, as shown by immunostaining and immunoblotting (Fig. 2, A and B). In p150CAF-1–depleted cells, we found that HP1α accumulation on local damage areas was strongly impaired (Fig. 2 C, middle). We reproducibly observed this defect in HP1α accumulation after p150CAF-1 depletion for exogenous GFP-mHP1α (Fig. S5, A and B) and for the other HP1 isoforms (Fig. S4 B). Moreover, p150CAF-1 depletion also impaired KAP-1 recruitment to damage sites (Fig. 2 C, middle) and the depletion of HP1α or KAP-1 reciprocally impaired their accumulation at damage sites without affecting p150CAF-1 accumulation (Fig. 2 D). Interestingly, neither HP1α nor p150CAF-1 recruitment was impaired by p60CAF-1 depletion (Fig. 2, C and D, right). Thus, p150CAF-1 itself, but not the complete CAF-1 complex, proved critical for the loading of HP1α (along with the other HP1 isoforms and KAP-1) onto damaged DNA.

Because p150CAF-1 and HP1α can interact directly (Murzina et al., 1999; Thiru et al., 2004), we tested whether this interaction was necessary for HP1α recruitment to damaged DNA. For this, we exploited a previously described strategy (Quivy et al., 2008) to deplete endogenous human p150CAF-1 with a siRNA against its 3′ untranslated region (UTR) and rescue p150CAF-1 expression with exogenous GFP-mp150CAF-1 mutants (Fig. 3 A). The selected p150CAF-1 mutants carry a deletion (ΔPVVVL) or a point mutation (V224D) in their PxVxL motif, shown to be critical for the interaction of p150CAF-1 with HP1 (Murzina et al., 1999). We verified that depletion of p150CAF-1 using the 3′ UTR siRNA effectively impaired HP1α accumulation at damage sites (Fig. 3, B and C). The rescue of p150CAF-1 expression with wild-type (wt) GFP-mp150 perfectly restored the accumulation of HP1α at damage sites (Fig. 3 C). Remarkably, however, neither ΔPVVVL nor V224D GFP-mp150 mutants were able to restore HP1α accumulation (Fig. 3 C), which demonstrates that the integrity of the HP1 binding site in p150CAF-1 is critical for HP1α recruitment to damaged DNA.

p150CAF-1, HP1α, and KAP-1 are involved in early and late steps of the DDR

To study how the recruitment of p150CAF-1 and HP1 proteins impacts upon the DDR, we performed siRNA-mediated depletion of p150CAF-1, HP1α, or KAP-1 in human U2OS cells and examined the activation of the DDR after DNA damage. As the phosphorylation of H2AX occurred normally in p150CAF-1–, HP1α–, and KAP-1–depleted cells (Fig. 2), we turned our attention to two downstream DDR factors, MDC1 and 53BP1 (FitzGerald et al., 2009; Bekker-Jensen and Mailand, 2010). In all three cases, the recruitment of MDC1 at localized laser-induced lesions occurred normally (Fig. 4 A). Conversely, p150CAF-1, HP1α, and KAP-1 depletion impaired the accumulation of 53BP1 at DNA damage sites (Fig. 4 B). This was not the case for p60CAF-1 depletion, further emphasizing the unique importance of p150CAF-1, but not the complete CAF-1 complex, in these early DDR events. To rule out off-targets effects of the siRNA against HP1α used (siHP1α No. D1), we confirmed that the recruitment of 53BP1 was impaired with another siRNA against HP1α (siHP1α No. S1 in Fig. S5, C–E). We also confirmed by immunoblotting that the effect of HP1α and KAP-1 depletion on 53BP1 recruitment was not simply caused by a reduction in 53BP1 protein level (unpublished data). To validate these findings in a quantitative manner, we counted the percentage of cells containing more than five 53BP1 IR-induced foci (Fig. 5, A and B). Together, these data argue that p150CAF-1, HP1α, and KAP-1 act early in the DDR cascade downstream of MDC1 but upstream of 53BP1.

We next examined consequences at later steps in the DDR, upon p150CAF-1 or HP1α depletion. Although the appearance of γH2AX and 53BP1 foci reflects DDR activation, their disappearance is generally considered as a means to monitor DSB repair kinetics (Rogakou et al., 1998, 1999; Schultz et al., 2000). We found that p150CAF-1 or HP1α depletion reduced the number of 53BP1 foci detectable at any time point after IR (Fig. 5, A and B), which suggests that p150CAF-1 and HP1α are required for either the recruitment or the retention of 53BP1 at DNA

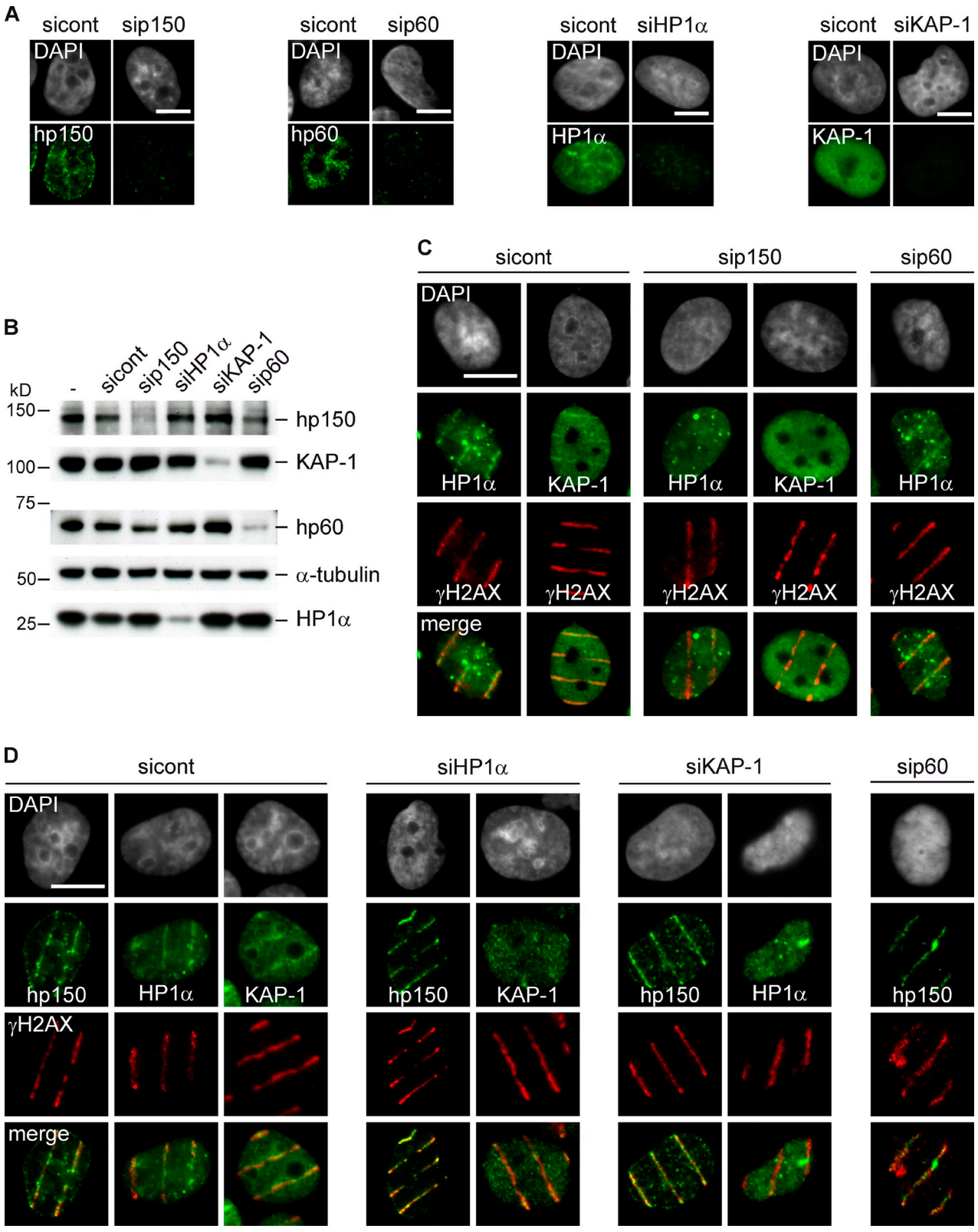

Figure 2. **p150CAF-1–dependent corecruitment of HP1α and KAP-1 to laser-induced DNA lesions.** (A and B) Confirmation of siRNA-mediated knockdown. We checked by immunostaining (A) and immunoblotting (B) the efficiency of depletion by using antibodies against human p150CAF-1 (hp150), human p60CAF-1 (hp60), HP1α, and KAP-1. We used α-tubulin as a loading control. (C) p150CAF-1-dependent recruitment of HP1α and KAP-1 to laser-induced DNA damage sites. We transfected U2OS cells with control siRNA against GFP (sicont), p150CAF-1 (sip150), or p60CAF-1 (sip60). 72 h later, we treated the cells as in Fig. 1 D, with CSK + Triton X-100 permeabilization and fixation within 5 min after a local laser irradiation. We performed immunostaining with antibodies against HP1α, KAP-1, and γH2AX. (D) Co-dependence of HP1α and KAP-1 recruitment to laser-induced DNA damage. We treated U2OS cells as previously, except that we used siRNA against HP1α (siHP1α) and KAP-1 (siKAP-1). Then, we performed immunostaining with antibodies against p150CAF-1, HP1α, KAP-1, and γH2AX. DNA was stained with DAPI. Bars, 10 μm.

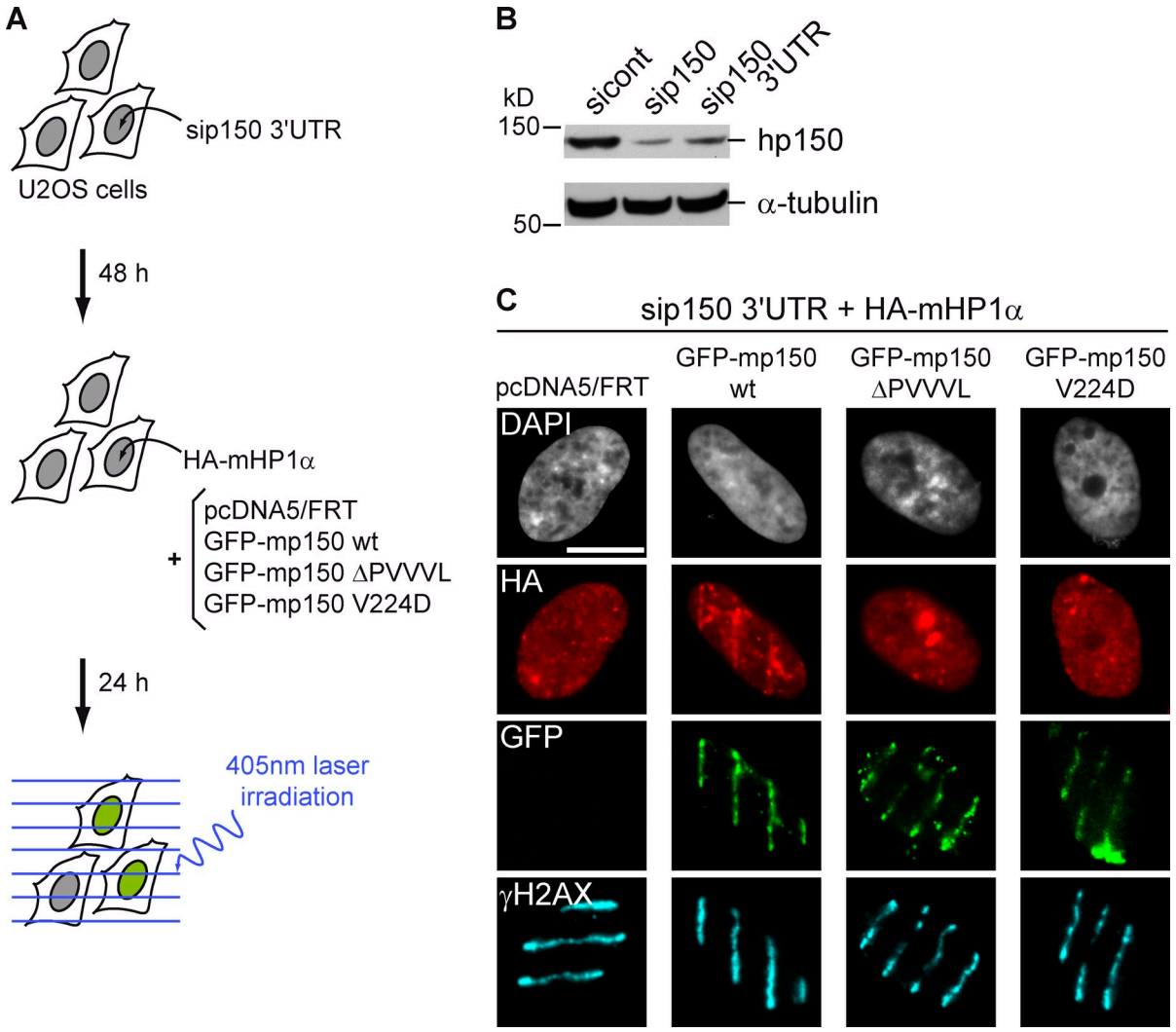

Figure 3. **Recruitment of HP1α to laser-induced DNA lesions through its interaction with p150CAF-1.** (A) Experimental scheme. We transfected U2OS cells with an siRNA specifically designed against the 3′ UTR of hp150CAF-1 (sip150 3′ UTR). 48 h later, we cotransfected pcDNA5/FRT+HA-mHP1α plasmid with GFP-mp150 wt or mutated in its PxVxL motif (ΔPVVVL and V224D mutants). The following day, we performed CSK + Triton X-100 permeabilization and fixation within 5 min after a local laser microirradiation. (B) Confirmation of siRNA-mediated knockdown. We checked by immunoblotting the efficiency of depletion of the siRNA against the 3′ UTR in comparison with the siRNA used in the rest of the experiments, after 48 h of transfection, using α-tubulin as a loading control. (C) Recruitment of HP1α to local laser-induced DNA damage via p150CAF-1. We treated cells as in A, performed immunostaining with antibodies against HA and γH2AX, and visualized p150CAF-1 by the direct detection of the GFP signal. DNA was stained with DAPI. Bars, 10 µm.

damage sites. Moreover, 5 min after IR, all cells showed an increase in the number of γH2AX foci, yet these foci did not disappear with the same kinetics at later time points in p150CAF-1– or HP1α-depleted cells (Fig. 5, A and C). Collectively, these observations argue for a defect in DSB repair. This prompted us to examine sensitivity to IR in comparison with the depletion of two proteins related to DSB repair, RAD51 and FANCD2 (Taniguchi et al., 2002). Our data show that both p150CAF-1– and HP1α-depleted cells exhibited a remarkable hypersensitivity to IR, which is comparable to that observed for depletions of other DSB repair proteins (Fig. 5, D and E).

p150CAF-1, HP1α, and KAP-1 influence HR-mediated DNA repair

To further explore the biological relevance of p150CAF-1 and HP1α for DSB repair, we analyzed how p150CAF-1, HP1α, and KAP-1 depletion affected the accumulation of proteins involved in each of the two major DSB repair pathways. We specifically chose to follow XRCC4, the cofactor of DNA ligase IV responsible for the ligation step in NHEJ, and RAD51, the recombinase responsible for the homology search and strand pairing steps in HR (Wyman and Kanaar, 2006). Although the accumulation of XRCC4 was not affected by depletion of p150CAF-1, HP1α, or KAP-1 (Fig. S5 F), the recruitment of RAD51 to sites of laser microirradiation at early time points was clearly impaired (Fig. 6 A). All siRNA-treated cells expressed similar levels of RAD51 proteins (Fig. 5, E and 6 D), arguing against an indirect effect caused by a reduction in RAD51 protein levels. We then focused on how HP1α might influence HR-mediated DNA repair. We used an I-SceI–based HR assay, and, as a positive control for HR impairment, we depleted C-terminal binding protein interacting protein (CtIP),

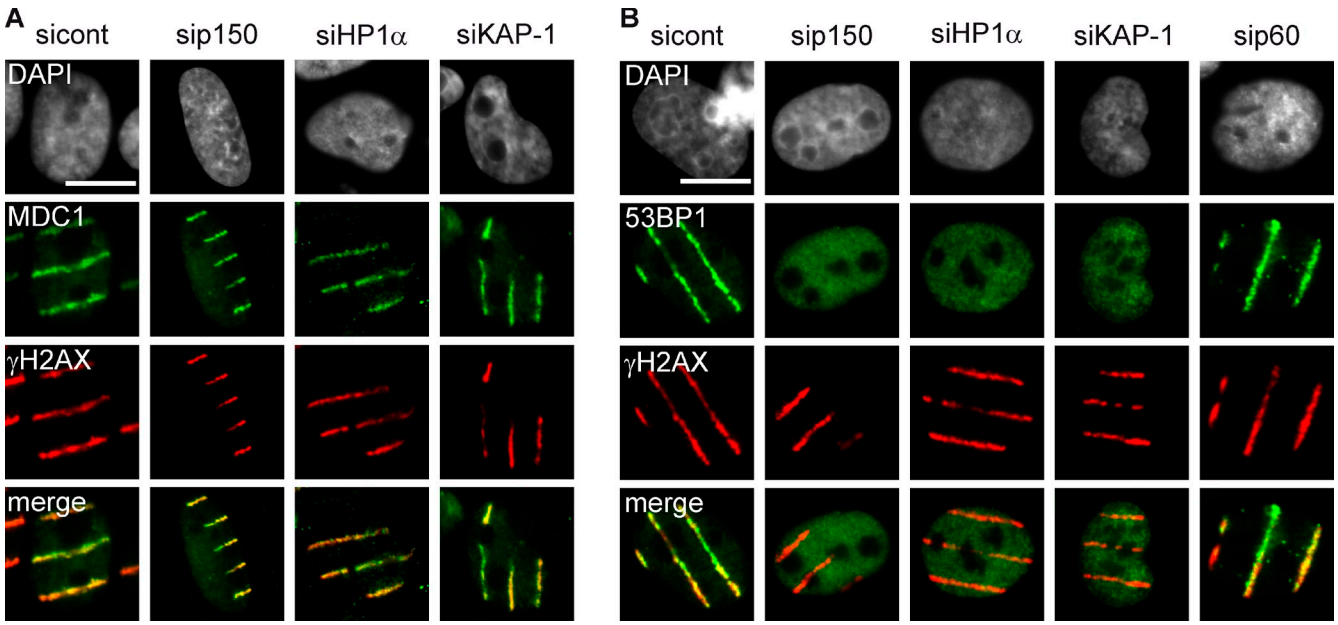

Figure 4. **53BP1 recruitment to laser-induced DNA damage is impaired by the depletion of p150CAF-1, HP1α, and KAP-1.** (A) MDC1 recruitment is not altered upon depletion of p150CAF-1, HP1α, or KAP-1. We transfected U2OS cells with the indicated siRNA and treated the cells as in Fig. 2 C, and we subsequently performed immunostaining with antibodies against MDC1 and γH2AX. (B) Defective recruitment of 53BP1 to DNA damage sites after depletion of p150CAF-1, HP1α, or KAP-1. We treated U2OS cells as in A and we performed coimmunostaining with antibodies against 53BP1 and γH2AX. DNA was stained with DAPI. Bars, 10 µm.

a critical protein for the initial steps of HR (Pierce et al., 2001; Sartori et al., 2007). Remarkably, HP1α-depleted cells exhibited a strong reduction in HR-mediated gene conversion without detectable effects on the cell cycle profile (Fig. 6, B and C). Although p150CAF-1 and KAP-1 depletion also lead to statistically significant decreases in HR efficiency ($P = 0.01$), one should be cautious when interpreting these data, as depletion of both proteins lead to substantial defects in cell cycle progression (Fig. 6 C and previous work). Indeed, given the fact that HR occurs in S and G2 phases, the observed repair efficiency might be an over- or underestimation of the real efficiency if corrected for cell cycle changes.

To gain further insight into how HP1α regulates HR-mediated DNA repair, we decided to explore if HP1α depletion might impair the end-resection step of HR, which is critical for the generation of single-stranded DNA and the sequential loading of RAD51. To test this, we followed the hyperphosphorylation of the N terminus of RPA2, an event that was previously linked to efficient DNA end resection (Sartori et al., 2007) and that occurs before RAD51 loading (Wyman and Kanaar, 2006). We treated HP1α-depleted U2OS cells with camptothecin (Fig. 6 E), which generates DSBs in S phase that are repaired by HR (Pommier et al., 2003). Notably, we observed that HP1α depletion impairs the phosphorylation of RPA2 to an extent that compares to the one observed after CtIP depletion, a protein reported to promote DNA end resection (Sartori et al., 2007). To further explore the potential link of HP1α in the resection step, we then focused on BRCA1. BRCA1 forms a complex with CtIP (Yu and Chen, 2004; Chen et al., 2008; Yu et al., 1998), which was recently proposed to stimulate DNA end resection (Bunting et al., 2010). We found a partial impairment (in ∼50% of the cells analyzed) in the recruitment of BRCA1 to DNA damage sites induced by laser microirradiation (Fig. 6 F). These observations are in line with the impaired recruitment observed for RAD51 (Fig. 6 A) and provide a first hint into the mechanism by which HP1α might regulate HR-mediated DNA repair. Together, these data evidence a direct involvement of HP1α in DNA repair by HR.

Discussion

In this study, by focusing on HP1α dynamics after DNA damage induction in both euchromatin and heterochromatin, we reveal that HP1α is an integral component of the DDR pathway. We provide the first mechanistic insight into how HP1α is recruited de novo to DNA damage sites by showing that its accumulation depends on the large subunit of the chromatin assembly factor 1, p150CAF-1. Moreover, we unveil a novel role of HP1α in DNA repair to promote early DDR events, which impacts upon the efficiency of HR repair.

Dependence on p150CAF-1 for recruitment of HP1α to DNA damage sites

By inflicting DNA damage in both chromatin domains, we observed that HP1α accumulates at sites of damage in both euchromatin and heterochromatin, and that in heterochromatin this recruitment is preceded by expansion of the HP1α domain at very early time points (Fig. 1 B). Our knockdown experiments show that the efficient accumulation of HP1 at damage sites depends on p150CAF-1 (Figs. 2 C and S4 B), and, most importantly, that the PxVxL interaction domain of p150CAF-1 is critical for HP1α recruitment (Fig. 3). In this respect, the

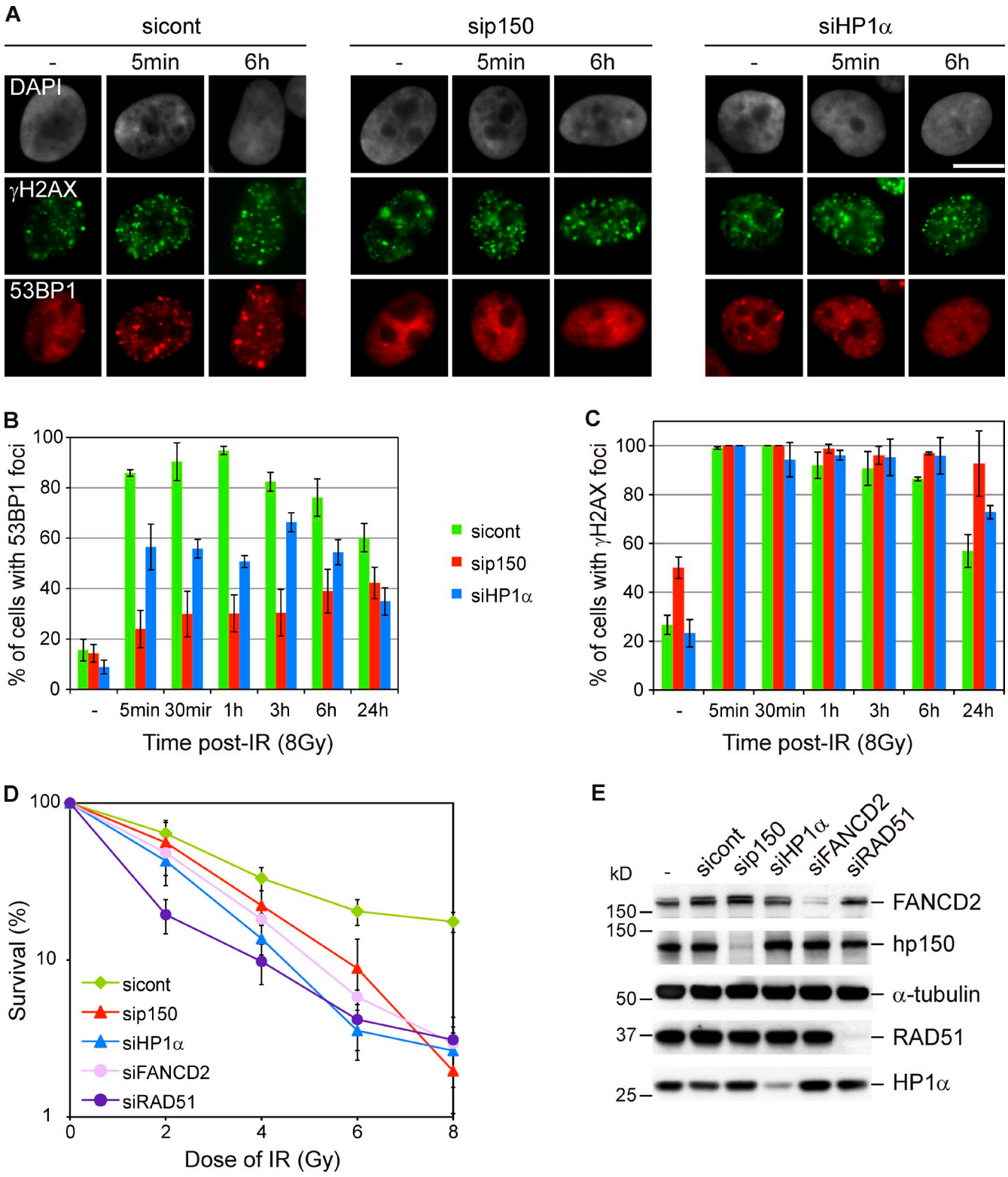

Figure 5. **Depletion of p150CAF-1 or HP1α leads to defects in the DDR and cell survival.** (A) Efficient formation of 53BP1 foci requires p150CAF-1 and HP1α. We transfected U2OS cells with the indicated siRNAs and, 72 h later, irradiated the cells with a dose of 8 Gy. At the indicated time after IR, we permeabilized the cells with CSK + Triton X-100 before fixation and performed coimmunostainings with anti-γH2AX and 53BP1 antibodies. DNA was stained with DAPI. Bars, 10 µm. (B and C) Percentage of cells with 53BP1 or γH2AX foci. Each value shown corresponds to the percentage of cells containing at least five foci of 53BP1 (B) or γH2AX (C) and represents the mean of three independent experiments. (D) IR sensitivity of p150CAF-1– and HP1α-depleted cells. We transfected U2OS cells with the indicated siRNA and analyzed their colony forming capacity after different doses of IR. Each value shown corresponds to the percentage of survival relative to the control and represents the mean of at least two experiments. The error bars represent the standard deviation of the mean. (E) Confirmation of siRNA-mediated depletion. On cells derived from this experiment, we performed immunoblotting to check the efficiency of depletions by using antibodies against hp150, HP1α, FANCD2, and RAD51, and we used α-tubulin as a loading control.

requirement of the chromoshadow domain in HP1 to ensure accumulation at DNA damage sites (Luijsterburg et al., 2009) is particularly interesting, as this is the exact same domain in HP1 that interacts with the PxVxL motif of p150CAF-1 (Murzina et al., 1999; Ryan et al., 1999; Thiru et al., 2004). Interestingly, in the context of replication and histone deposition, p150CAF-1 recruitment at sites of DNA synthesis is thought to use PCNA as a landing platform (Shibahara and Stillman, 1999; Moggs et al., 2000; Rolef Ben-Shahar et al., 2009). It is therefore tempting to speculate that HP1α recruitment to repair sites might exploit a similar mechanism. However, p150CAF-1 accumulation precedes the step in which PCNA is actually required for DNA synthesis during HR (Wyman and Kanaar, 2006). Notably, previous studies showed nevertheless that PCNA gets efficiently recruited as early as 2 min after laser-induced damage (Hashiguchi et al., 2007; Mortusewicz and Leonhardt, 2007), although the exact role for such a rapid accumulation had remained unclear so far. Therefore, our findings may provide functional relevance for this early PCNA loading to promote p150CAF-1 recruitment to damage sites.

Another important point to stress based on our observations is that HP1 accumulation at damage sites occurs early in the DDR and rapidly disappears (Figs. 1 E and S4 A), which suggests that its retention on damaged DNA is tightly controlled. Given that KAP-1 is known to promptly leave DNA damage sites after its phosphorylation by ATM (Ziv et al., 2006) and that our data shows that the retention of HP1α at damage sites requires KAP-1, we hypothesize that HP1α release from damage sites might be linked to the ATM-dependent phosphorylation of KAP-1. In addition, it is also possible that other chromatin modifications at damaged sites (van Attikum and Gasser, 2009) could contribute to the release of HP1α. Conversely, HP1 might simply be unable to be retained at damage sites unless H3K9me3 is imposed by the SUV39 enzyme. This possibility is consistent with our observations (Fig. S4, C and E). Furthermore, for the release of HP1 to take place effectively, somehow the initial interaction with p150CAF-1 should be disrupted, as CAF-1 stays for a longer time frame at damage sites. Given that the HP1α complexes isolated from cells contain CAF-1 but not histones, and that histone H3.1 complexes retrieve CAF-1 but not HP1α (Quivy et al., 2004; Loyola et al., 2009), an intriguing possibility that might explain why HP1 is no longer retained by CAF-1 is that p150CAF-1 function switches toward an active histone chaperone mode as a part of the CAF-1 complex. In this way, CAF-1 would ensure the restoration of the chromatin organization at the end of DNA repair (Green and Almouzni, 2003; Polo et al., 2006; Groth et al., 2007b; Polo and Almouzni, 2007). Collectively, these findings reveal that, in addition to its known functions in histone deposition, p150CAF-1 plays an independent role at early steps of the DDR to promote the recruitment of HP1 to DNA damage sites.

The novel role of HP1 in HR-mediated repair

We observed that HP1α depletion leads to the impairment of 53BP1, BRCA1, and RAD51 accumulation at damage sites (Figs. 4–6). It is surprising that although many studies link 53BP1 to NHEJ (Xie et al., 2007; Difilippantonio et al., 2008; Dimitrova et al., 2008; Bunting et al., 2010), we did not observe defects in XRCC4 recruitment (Fig. S5 F). Although our initial analysis using a random plasmid integration assay that measured the end joining efficiency in the absence of DNA damage (Stucki et al., 2005) suggests that HP1α depletion has no effect on NHEJ (unpublished data), further work is needed to analyze HP1α impact on NHEJ in the presence of chromatin-localized DNA damage. Because 53BP1 is also linked to several processes related to DNA damage signaling (FitzGerald et al., 2009), our data rather implies that the role of HP1α in 53BP1 recruitment might be to promote early DDR signaling. Remarkably, however, HP1α depletion leads to substantial defects in HR (Fig. 6). Although several previous studies have implicated different p150CAF-1 homologues in recombinational repair (Lewis et al., 2005; Song et al., 2007; Ishii et al., 2008), our work is the first to attribute an active role for the p150CAF-1–HP1α complex in HR. Interestingly, a previous study argues for a negative role of HP1 in DNA repair, based on data using simultaneous depletion of the three HP1 isoforms to show that this can overcome the defect of ATM-inhibited cells to repair heterochromatic DSBs (Goodarzi et al., 2008). Although this may appear to be in apparent contrast with our findings, we should stress that our results do not exclude the possibility that massive chromatin relaxation after depletion of all HP1 isoforms renders the heterochromatin domain prone to repair, but on the contrary establish that a specific HP1 isoform, HP1α, has an active role in DNA repair. Thus, dual roles for HP1 proteins have to be considered.

The outstanding question is by which mechanism HP1α accumulation promotes HR. An intriguing possibility would be that transient HP1α binding to damaged chromatin, independent of HP1α interaction with heterochromatin marks, helps to stabilize loose ends and keep sister chromatids in proximity after the induction of DSBs. This idea of binding DNA molecules "in trans" is supported by HP1 involvement in sister chromatid cohesion (Inoue et al., 2008). However, this model does not explain how HP1 could directly promote the accumulation of RAD51 at damage sites, as the formation of the RAD51 filament precedes the homology search step (Holthausen et al., 2010). Our data rather suggest that HP1α might stimulate a step upstream in the HR pathway. A logical candidate would be the DNA end-resection step that is required for RAD51 loading. In line with this possibility, we find that RPA2 phosphorylation, a modification associated with DNA end resection, is affected by HP1α depletion (Fig. 6 E). Because CtIP, a critical protein for the resection step, is recruited to laser damage sites with a similar kinetics to the one we observe for HP1α (Sartori et al., 2007), and HP1α and CtIP depletion lead to similar levels of impairment in RPA2 phosphorylation (Fig. 6 E), we envisage that HP1α accumulation might be relevant to promote CtIP recruitment to damage sites. This hypothesis is further supported by our observation that the recruitment of BRCA1, a known partner of CtIP (Yu et al., 1998; Chen et al., 2008), is partially affected (Fig. 6 F). Future work will be required to dissect the potential interrelationships between BRCA1, CtIP, and HP1α during HR-mediated repair.

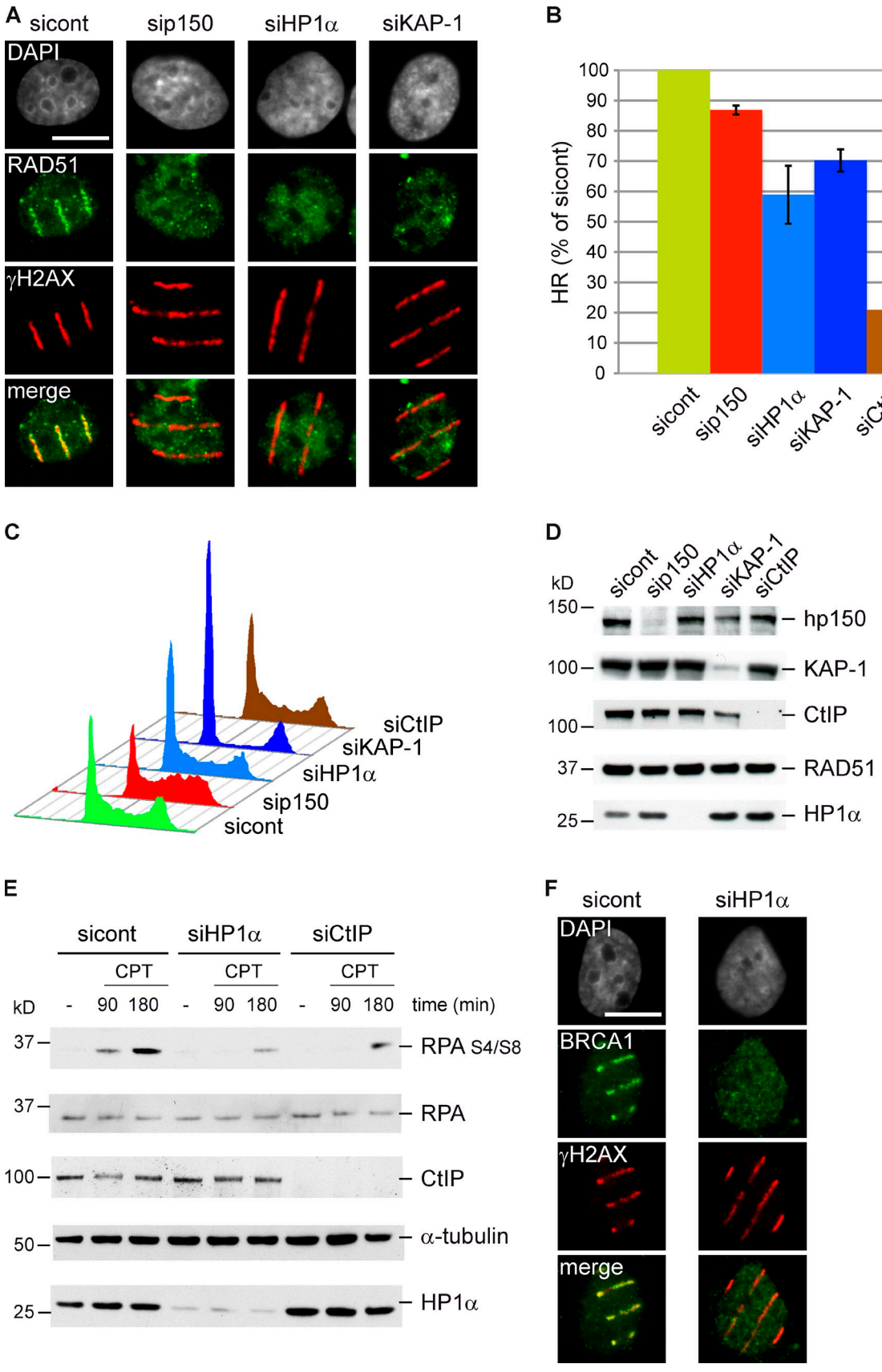

Figure 6. **HR-mediated DSB repair is impaired by depletion of p150CAF-1, HP1α, and KAP-1.** (A) Defective recruitment of RAD51 after depletion of p150CAF-1, HP1α, or KAP-1. We transfected U2OS cells with the indicated siRNAs and treated the cells as in Fig. 2 C, with CSK + Triton X-100 permeabilization and fixation within 5 min after laser-induced DNA lesions. We subsequently performed immunostaining with antibodies against RAD51 and γH2AX. DNA was stained with DAPI. Bars, 10 µm. (B) HR-mediated gene conversion is impaired after depletion of p150CAF-1, HP1α, or KAP-1.

Together, this manuscript provides strong arguments that put forward HP1α as an active player in early DNA damage signaling and specific repair pathways. Thus, HP1α should not be considered merely as an obstacle for DNA repair but also as an important component of HR. This conceptual advance should broaden our understanding of the complex cellular function of HP1α.

Materials and methods

Cell lines, culture, and transfection

We used mouse cells: NIH 3T3 (American Type Culture Collection No. CRL-1658; Maison et al., 2002) and *Suv39h* double-null mouse embryonic fibroblasts (MEFs; provided by T. Jenuwein, Max Planck Institute of Immunobiology and Epigenetics, Freiburg, Germany; Peters et al., 2001; Maison et al., 2002); and human cells: U2OS (provided by J. Bartek, Institute of Cancer Biology and Centre for Genotoxic Stress Research, Copenhagen, Denmark; Groth et al., 2007a), U2OS+DR-GFP (provided by M. Jasin, Sloan-Kettering Institute, New York, NY), HeLa (provided by P. Cook, Sir William Dunn School of Pathology, University of Oxford, Oxford, England, UK; Kimura and Cook, 2001), and XP-G cells, XP3BR (provided by A. Sarrasin, Institut Gustave Roussy, Villejuif, France; Green and Almouzni, 2003; Polo et al., 2006). We cultured these cells in DME (Invitrogen) supplemented with 10% (vol/vol) FCS (Eurobio), 100 U/ml penicillin, and 100 µg/ml streptomycin (Invitrogen) in a humidified atmosphere with 5% CO_2 at 37°C. We maintained U2OS+DR-GFP cells in medium supplemented with 1 µg/ml puromycin (Invitrogen). We also used mouse Flp-In 3T3 cells (Invitrogen) and Flp-In 3T3+GFP-mp150 cells, which stably express GFP-mouse p150CAF-1 fusion proteins (Quivy et al., 2008). For these cells, we completed the medium with donor calf serum (DCS; Biowest) instead of FCS and supplemented it with 100 µg/ml zeocin (Invitrogen) for Flp-In 3T3 cells and with 150 µg/ml hygromycin (Roche) for Flp-In 3T3+GFP-mp150 cells.

We transfected 1 µg of plasmid into mouse cells at 30–40% confluency with Effecten (QIAGEN) or human cells at 50–70% confluency with Lipofectamine 2000 (Invitrogen) and 30–100 nM siRNA duplexes into human cells at 20–30% confluency with Lipofectamine RNAiMAX (Invitrogen). We performed transfections in 30/60-mm dishes according to the respective manufacturers' instructions. We performed subsequent experiments 24–48 h after plasmid transfection and 48–72 h after siRNA transfection.

Plasmids

To generate GFP-tagged mouse HP1α (GFP-mHP1α) expression plasmids, we amplified by PCR the mHP1α cDNA from the pGEX-2T+mHP1α plasmid (a gift of R. Losson, Institut de Génétique et de Biologie Moléculaire et Cellulaire, Illkirch, France; Le Douarin et al., 1996) with forward and reverse primers, 5′-AAAA**CTCGAG**ATGGGAAAGAAGACCAAGAGGACAGCCGACA-3′ and 5′-AAAA**CTGCAG**TTAGCTCTTCGCGCTTTCTTTTTCTTTGTT-3′, containing XhoI and PstI restriction sites (shown in bold). After digestion with XhoI and PstI enzymes, we ligated the mHP1α PCR product into XhoI- and PstI-digested peGFP-C3 vector (Takara Bio Inc.). We subcloned the GFP-mHP1α fragment, obtained by cutting the peGFP+mHP1α plasmid with NheI and BamHI enzymes, into NheI- and BamHI-digested pcDNA5/FRT vector (Invitrogen). We verified the peGFP+mHP1α and pcDNA5/FRT+GFP-mHP1α plasmids by sequencing.

We also used previously characterized plasmids, such as peGFP+hp150 (Green and Almouzni, 2003), pcDNA5/FRT+HA-mHP1α (Maison et al., 2011), pcDNA5/FRT+GFP-mp150 wt, pcDNA5/FRT+GFP-mp150 ΔPVVVL, and pcDNA5/FRT+GFP-mp150 V224D (Murzina et al., 1999; Quivy et al., 2008). The last two plasmids contain mp150CAF-1 constructs, respectively deleted and mutated in the PxVxL motif.

siRNA sequences

The sequences of the siRNA duplexes used (Thermo Fisher Scientific) were as follows: sip150, 5′-GGAGAAGGCGGAGAAGCAG-3′ (Quivy et al., 2004); sip150 3′ UTR, 5′-TATATAGGATGCTGGATTA-3′; sip60, 5′-AAUCUUGCUCGUCAUACCAAA-3′ (Polo et al., 2006); siHP1α, 5′-GGGAGAAGUCAGAAAGUAA-3′ (#D1), used in almost all experiments, and 5′-CCUGAGAAAAACUUGGAUUTT-3′ (#S1; Obuse et al., 2004; De Koning et al., 2009); siGENOME siKAP-1, 5′-GCGAUCUGGUUAUGUGCAA-3′ (D-005046-05, #5) and 5′-AGAAUUAUUUCAUGCGUGA-3′ (D-005046-06, #6), which were used indifferently; siCtIP, 5′-GCUAAAACAGGAACGAAUC-3′ (Sartori et al., 2007; Yu and Chen, 2004); ON-TARGETplus SMARTpool siFANCD2 (L-016376), 5′-UGGAUAAGUUGUCGUCUAU-3′, 5′-CAACAUACCUCGACUCAUU-3′, 5′-GGAUUUACCUGUGAUAATA-3′, and 5′-GGAGAUUGAUGGUCUACUA-3′; siXRCC4, 5′-AUAUGUUGGUGAACUGAGA-3′ (Ahnesorg et al., 2006); ON-TARGETplus SMARTpool siRAD51 (L-003530), 5′-UAUCAUCGCCCAUGCAUCA-3′, 5′-CUAAUCAGGUGGUAGCUCA-3′, 5′-GCAGUGAUGUCCUGGAUAA-3′, and 5′-CCAACGAUGUGAAGAAAUU-3′; and sicont, 5′-GCUGGAGUACAACUACAAC-3′ (Quivy et al., 2004). The referred sicont targets the RNA sequence of GFP and serves as control siRNA in all experiments. However, when indicated, we used another control siRNA, the ON-TARGETplus Nontargeting siRNA (D-001810-01-05).

DNA damage induction

When necessary, we used glass coverslips coated with a solution of 20 µg/ml collagen and 1 µg/ml fibronectin (Sigma-Aldrich) in PBS (Invitrogen) for 1 h at 37°C, rinsed three times in PBS. We seeded cells at a density chosen according to the further processing (see the Cell lines, culture, and transfection paragraph) the evening before.

Camptothecin. We treated cells with 1 µM camptothecin (Sigma-Aldrich) and harvested them at the indicated time point.

UV light radiation. We performed local UV-C irradiation through an Isopore 5.0 µm pore filter (TMTP01300; Millipore) or an Isopore 8.0-µm pore filter (TETP09030; Millipore) using a low-pressure 254-nm mercury lamp (dose rate: 5 J/m^2/s) or a UV cross-linker (Stratalinker 1800; Agilent Technologies) as described previously (Moné et al., 2001; Gérard et al., 2006; Soria et al., 2009).

IR. We applied a dose of 8 Gy using a ^{137}Cs source (dose rate: 0.96 Gy/min). After washing coverslips twice in PBS, we placed them in fresh medium at 37°C for postirradiation incubation. As a control, we used mock samples, which we treated exactly in the same way with the exception of irradiation.

Laser-induced damage. To generate localized DNA lesions, we used as the main technique in this work a method described previously (Rogakou et al., 1999), with some modifications. We presensitized the cells with 10 µg/ml viable Hoechst dye 33258 (Sigma-Aldrich) for 5 min at 37°C, without 24 h of pretreatment with 0.4 µM BrdU and 2.4 µM thymidine. We performed laser microirradiation by using an inverted confocal microscope (LSM 510 Meta; Carl Zeiss, Inc.) equipped with a 37°C heating chamber and a 25-mW 405 nm diode laser focused through a 63× Plan-Apochromat/1.4 NA oil objective. We set the laser output to 70% of maximum power to generate in one scan detectable DNA damage restricted to the laser path in a presensitization-dependent manner without noticeable cytoxicity. To target a large number of nuclei, we scanned several adjacent fields with the 405 nm laser in a pattern of evenly spaced parallel lines, generating a "cylinder of damage" <1 µm in diameter through the nuclei. After two washes with PBS, we reincubated the coverslips in fresh medium

We analyzed the frequency of HR-mediated DNA repair events in U2OS+DR-GFP cells transfected with the indicated siRNAs. Each value shown corresponds to the percentage of HR relative to the control (sicont) and represents the mean of three independent experiments. The error bars represent the standard deviation of the mean. (C) Cell cycle profile of siRNA-transfected cells. In parallel, we monitor the cell cycle status of the siRNA-treated cells by flow cytometry analysis. (D) Confirmation of siRNA-mediated depletion. We performed immunoblotting to confirm that the indicated siRNA-mediated depletions were efficient in experiments from B. We used RAD51 as loading control. (E) Phosphorylation of the middle subunit of RPA is affected after depletion of HP1α. We transfected U2OS cells with the indicated siRNAs. 48 h later, we treated the cells with 1 µM camptothecin (CPT). At the indicated time points, we harvested the cells and performed immunoblotting with antibodies against RPA32, RPA32 S4/S8, HP1α, and CtIP. We used α-tubulin as loading control. (F) Defective recruitment of BRCA1 after depletion of HP1α. We transfected U2OS cells with the indicated siRNAs and treated the cells as in Fig. 2 C, with CSK + Triton X-100 permeabilization and fixation within 5 min after laser irradiation. We subsequently performed immunostaining with antibodies against BRCA1 and γH2AX. DNA was stained with DAPI. Bars, 10 µm.

at 37°C and fixed the cells at the indicated time points for immunofluorescence (IF) analysis. For single nuclei imaging, we induced DNA damage in a restricted region with a width of 2 µm by applying three iterations of the 405 nm laser with 100% power, and we took serial time-lapse images at 3% power of the 488-nm line from a 200 mW argon laser with laser current set at 6.1 Å.

For all DNA damage induction, we performed three independent experiments.

Clonogenic cell survival assays

We determined the sensitivity of siRNA-treated U20S cells to increasing doses of IR by measuring their colony forming ability, as described previously (Essers et al., 1997). In brief, we plated 1,000 cells onto 60-mm dishes, and after 12–16 h, we exposed the cells to the appropriate doses of IR (0–8 Gy) using a ^{137}Cs source (dose rate: 0.96 Gy/min). After two washes in PBS, we placed the cells in fresh medium and left them growing for 10 d to allow colony formation. We then fixed, stained by Coomassie, and counted the colonies. We performed all experiments in triplicate and presented the results depicted on a logarithmic scale normalized to plating efficiencies.

Cell cycle analysis by flow cytometry

We performed cell cycle analysis as described previously (Soria et al., 2008). In brief, we collected siRNA-treated cells by trypsinization using the same culture media to avoid loosing detached cells. Then, we pelleted the cells by centrifugation at 500 *g* and we immediately fixed them in ice-cold ethanol with gentle vortexing. After a minimum of 2 h at −20°C, we pelleted the cells and resuspended them in PBS containing 50 µg/ml propidium iodide and 50 µg/ml RNase. We collected the samples using a C6 flow cytometer (Accuri) and analyzed them using FlowJo software (TreeStar Inc.). We analyze a minimum of 10,000 cells/sample.

HR assay

We used an HR assay generated previously in U2OS cells containing an integrated HR reporter substrate DR-GFP (Pierce et al., 2001; Sartori et al., 2007), with some modifications. In brief, 48 h after siRNA transfection in 60-mm dishes, we cotransfected the U2OS+DR-GFP cells with pCBASce, a plasmid expressing the I-SceI endonuclease that initiates the HR event that will reestablish a full-length GFP sequence, and pCS2-mRFP, a plasmid expressing mRFP to follow the transfection efficiency (both plasmids provided by S. Jackson, Wellcome Trust/Cancer Research UK Gurdon Institute, University of Cambridge, Cambridge, England, UK). 2 d after I-SceI transfection, we harvested cells and performed flow cytometry analysis on C6 flow cytometer (Accuri) to determine HR-mediated DNA repair events induced by I-SceI digestion. We gated the live cell population by exclusion of dead cells stained with Sytox Red (Invitrogen) and we analyzed the mRFP-positive cell population to avoid possible differences caused by transfection efficiencies. We analyzed FACS data by using CFlow software to evaluate the percentage of GFP-positive cells relative to the number of mRFP-positive cells (HR levels). We showed the results normalized to control siRNA as a percentage of sicontrol.

Antibodies

Primary antibodies used during immunoblot (IB) or IF experiments are listed below. Rabbit anti-53BP1 (IB and IF, 1:500; NB 100-304; Novus Biologicals; Soutoglou et al., 2007); mouse anti–pyrimidine 6,4-pyrimidone photoproduct (6,4-PP; IF, 1:1,000; KTM50; Kamiya Biomedicals; Green and Almouzni, 2003; Polo et al., 2006) after 10 min of denaturation in 4 M HCl at RT before blocking; rabbit anti-ATM phospho-Ser1981 (IB and IF, 1:500; 600-401-398; Rockland; Bakkenist and Kastan, 2003); mouse anti-BRCA1 (IF, 1:500; Ab-1 [EMD] and ab16781 [Abcam]; Scully et al., 1996); rabbit anti–mouse p60CAF-1 (IF, 1:500; AgroBIO; Green and Almouzni, 2003); rabbit anti–human p60CAF-1 (IF, 1:250; AgroBIO; Green and Almouzni, 2003); rabbit anti–mouse p150CAF-1 (IF, 1:1,000; AgroBIO; Quivy et al., 2004); mouse anti–human p150CAF-1 (IB and IF, 1:1,000; ab7655; Abcam; Polo et al., 2006); mouse anti–cyclobutane pyrimidine dimer (CPD; IF, 1:2,000; KTM53; Kamiya Biomedicals; Green and Almouzni, 2003; Polo et al., 2006) after 5 min of denaturation in 0.5 M NaOH at RT before blocking; mouse anti-Chk1 (IB, 1:500; sc-8408; tebu-bio); rabbit anti-Chk1 phospho-Ser317 (IB, 1:1,000; 2344; Cell Signaling Technology; Groth et al., 2005; Quivy et al., 2008); mouse anti-Chk2 (IB, 1:500; ab3292; Abcam; Groth et al., 2005); rabbit anti-Chk2 phospho-Thr68 (IB, 1:1,000; 2661; Cell Signaling Technology; Lukas et al., 2003); mouse anti-CtIP (IB, 1:50; provided by R. Baer; Sartori et al., 2007); rabbit anti-FANCD2 (IB, 1:1,000; IF, 1:500; NB 100-182; Novus Biologicals; Garcia-Higuera et al., 2001; Bekker-Jensen et al., 2006); rabbit anti-FANCD2 (IB, 1:1,000; IF, 1:500; ab2187; Abcam; Bogliolo et al., 2007); mouse anti-GFP (IF, 1:500; 11 814 460; Roche; van Veelen et al., 2005); rabbit anti-GFP (IF, 1:1,000; 8372; Takara Bio Inc.); mouse anti–H2A-ub (IF, 1:500; 05-678; Millipore; Wang et al., 2004; Mailand et al., 2007); rat anti-HA (IF, 1:250; 11 867 431 001; Roche); mouse anti-γH2AX (IF- 1:2,000; 05-636; Millipore; Lukas et al., 2003); rabbit anti-γH2AX (1:500; 07-164; Millipore; Rogakou et al., 1999; Lukas et al., 2003); rabbit anti-H3K9me3 (IF, 1:500; 07-442; Millipore; Houlard et al., 2006; Loyola et al., 2009); mouse anti-HP1α (IF, 1:1,000; 2HP-1H5-AS; Euromedex; Maison et al., 2002); rabbit anti-HP1α (IB, 1:1,000; IF, 1:2,000; H-2164, Sigma-Aldrich; De Koning et al., 2009); mouse anti-HP1β (IF, 1:1,000; 1MOD-1A9; Euromedex; Quivy et al., 2004; De Koning et al., 2009); mouse anti-HP1γ (IF, 1:1,000; 2MOD-1G6; Euromedex; Quivy et al., 2004; De Koning et al., 2009); rabbit anti–KAP-1 (IB and IF, 1:500; A300-274; Bethyl Laboratories, Inc.; Ziv et al., 2006); goat anti-Ku80 (IF, 1:500; sc-1484; Santa Cruz Biotechnology, Inc.; Jin and Weaver, 1997; Mari et al., 2006); sheep anti-MDC1 (IF, 1:500; GTX 10948; GeneTex; Goldberg et al., 2003; Lou et al., 2003); rabbit anti-NBS1 phospho-Ser343 (IF, 1:500; NB 100-284; Novus Biologicals; Goodarzi et al., 2004); rabbit anti-p53 phospho-Ser15 (IB, 1:500; 9284; Cell Signaling Technology; Groth et al., 2005; Quivy et al., 2008); rabbit anti–human RAD51 (IB, 1:1,000; IF, 1:500; PC130; EMD; Soutoglou et al., 2007); rabbit anti-RPA32 (IB, 1:500; 691-P1ABX; Neomarkers); rabbit anti-RPA32 phospho-Ser4/Ser8 (IB, 1:1,000; A300-245A; Bethyl Laboratories Inc.); rabbit anti-XRCC4 (IF, 1:500; ab2857; Abcam; McManus and Hendzel, 2005); rabbit anti-XRCC4 (IB, 1:1,000; AHP387; Serotec; Drouet et al., 2005); and mouse α-tubulin (IB, 1:20,000; T 9026; Sigma-Aldrich), which was used as loading control. Secondary antibodies used were: for IB, HRP-conjugated affinity-purified sheep anti–mouse or donkey anti–rabbit (1:2,500; Jackson ImmunoResearch Laboratories, Inc.); and for IF, donkey anti–goat, anti–mouse, anti–rabbit, or anti–sheep coupled to Alexa Fluor 488 or 594 (1:1,000; Invitrogen).

Immunoblotting

We lysed the cells in EBC lysis buffer (50 mM Tris-HCl, pH 7.4, 150 mM NaCl, 0.5% Nonidet P-40, 0.5 mM EDTA, pH 8, and 1 mM β-mercaptoethanol) containing a cocktail of protease inhibitor (Complete, EDTA-free tablets; Roche). We clarified the lysates by centrifugation at 14,000 *g* before use in immunoblot analysis. We quantified the protein concentrations by the Bradford method (Bio-Rad Protein Assay; Bio-Rad Laboratories). For each extract, 15 µg of protein was separated on 10% SDS-PAGE and transferred onto nitrocellulose membranes (Protran). For visualization of proteins after Western blots with the indicated primary antibodies and the appropriate secondary antibodies, we used SuperSignal West Pico Chemiluminescent Substrate (Thermo Fisher Scientific) for chemiluminescence detection.

IF

Immunostaining. At indicated times after DSB induction, we performed immunostaining as described previously (Martini et al., 1998; Green and Almouzni, 2003; Quivy et al., 2004).

For in situ cell fractionation, we washed the coverslips twice in PBS, rinsed them with cytoskeleton buffer (CSK) containing 10 mM Pipes, pH 6.8, 100 mM NaCl, 300 mM sucrose, 3 mM $MgCl_2$, and a cocktail of protease inhibitor (Complete, EDTA-free tablets; Roche). We subsequently performed a Triton X-100 extraction by incubating the coverslips in CSK containing 0.5% Triton X-100 for 5 min on ice. After washes in CSK and PBS, we fixed cells with 2% wt/vol paraformaldehyde for 20 min at RT.

When necessary, before fixation, we performed an RNase treatment as described previously (Maison et al., 2002). In brief, we incubated Triton X-100–permeabilized cells in 3.5 mg/ml RNase A (5 U; USB) in PBS for 10 min at RT. We then rinsed the coverslips twice in PBS before fixation in paraformaldehyde.

For standard immunostaining, we washed the coverslips twice with PBS/0.1%T (PBS containing 0.1% vol/vol Triton X-100) and permeabilized the cells in PBS/0.1%T for 10 min at RT. After two washes with PBT (PBS containing 0.1% vol/vol Tween 20), we incubated the coverslips in 5% BSA in PBT for 5 min at RT and, subsequently, with the appropriate primary antibodies, diluted in blocking buffer for 90 min at RT. After three washes with PBT and one with blocking buffer, we incubated the coverslips with appropriate secondary antibodies for 45 min, washed them once in PBT, and incubated them with 0.5 µg/ml DAPI in PBT for 5 min. After two washes in PBT and a final rinse in PBS, we mounted samples onto slides in Vectashield mounting medium (Vector Laboratories).

Image acquisition. We used an epifluorescence microscope (Axio Imager Z1; Carl Zeiss, Inc.) piloted with MetaMorph software (Molecular Devices), a 63× PA/1.4 NA oil objective lens, and a chilled charge-coupled device camera (CoolSnap HQ^2; Photometrics) for image acquisition.

Online supplemental material

Fig. S1 shows a detailed characterization of the laser-induced damage method used in this study. Fig. S2 shows data on the recruitment of HP1α and P150CAF-1 across the cell cycle. Fig. S3 shows information regarding the link between HP1α recruitment and the DSB repair machinery. Fig. S4 presents data to show that both HP1β and HP1γ follow a similar recruitment/release timing to the one observed for HP1α, and that HP1α recruitment to DNA damage sites occurs in the absence of typical heterochromatin marks. Fig. S5 shows additional evidence of the dependence of HP1α recruitment on p150CAF-1 and KAP-1 and data showing the normal recruitment of the NHEJ ligase cofactor, XRCC4, after HP1α depletion. Online supplemental material is available at http://www.jcb.org/cgi/content/full/jcb.201101030/DC1.

We are grateful to S. Polo, E. Moustacchi, J-P. Quivy, and L. Prendergast for critical reading of the manuscript and to members of UMR218 for helpful discussions. We thank our anonymous reviewers for their constructive comments.

We greatly thank the PICT-iBiSA Imaging facility of Centre de Recherche de l'Institut Curie (F. Waharte and, especially P. Le-Baccon and O. Leroy). C. Baldeyron received support from Association pour la Recherche sur le Cancer, G. Soria from the program Research in Paris of the Mairie de Paris, and A.J. Cook from the National Health and Medical Research Council of Australia (2009-10, No. 471498). This work was supported by la Ligue Nationale contre le Cancer (équipe labelisée Ligue 2010), PIC Programs, the European Commission Network of Excellence Epigenome (LSHG-CT-2004-503433), the European Commission ITN FP7-PEOPLE-2007 "Image DDR" and FP7-PEOPLE-2008 "Nucleosome 4D", ACI-2007-Cancéropôle IdF "Breast cancer and Epigenetics," Agence Nationale pour la Recherche "ECenS" ANR-09-BLAN-0257-01, INCa "GepiG" and European Research Council Advanced grant 2009-AdG_20090506.

Submitted: 7 January 2011
Accepted: 7 March 2011

References

Ahnesorg, P., P. Smith, and S.P. Jackson. 2006. XLF interacts with the XRCC4-DNA ligase IV complex to promote DNA nonhomologous end-joining. *Cell*. 124:301–313. doi:10.1016/j.cell.2005.12.031

Ayoub, N., A.D. Jeyasekharan, J.A. Bernal, and A.R. Venkitaraman. 2008. HP1-beta mobilization promotes chromatin changes that initiate the DNA damage response. *Nature*. 453:682–686. doi:10.1038/nature06875

Ayoub, N., A.D. Jeyasekharan, and A.R. Venkitaraman. 2009. Mobilization and recruitment of HP1: a bimodal response to DNA breakage. *Cell Cycle*. 8:2945–2950.

Bakkenist, C.J., and M.B. Kastan. 2003. DNA damage activates ATM through intermolecular autophosphorylation and dimer dissociation. *Nature*. 421:499–506. doi:10.1038/nature01368

Bekker-Jensen, S., and N. Mailand. 2010. Assembly and function of DNA double-strand break repair foci in mammalian cells. *DNA Repair (Amst.)*. 9:1219–1228. doi:10.1016/j.dnarep.2010.09.010

Bekker-Jensen, S., C. Lukas, R. Kitagawa, F. Melander, M.B. Kastan, J. Bartek, and J. Lukas. 2006. Spatial organization of the mammalian genome surveillance machinery in response to DNA strand breaks. *J. Cell Biol.* 173:195–206. doi:10.1083/jcb.200510130

Bogliolo, M., A. Lyakhovich, E. Callén, M. Castellà, E. Cappelli, M.J. Ramírez, A. Creus, R. Marcos, R. Kalb, K. Neveling, et al. 2007. Histone H2AX and Fanconi anemia FANCD2 function in the same pathway to maintain chromosome stability. *EMBO J.* 26:1340–1351. doi:10.1038/sj.emboj.7601574

Bunting, S.F., E. Callén, N. Wong, H.T. Chen, F. Polato, A. Gunn, A. Bothmer, N. Feldhahn, O. Fernandez-Capetillo, L. Cao, et al. 2010. 53BP1 inhibits homologous recombination in Brca1-deficient cells by blocking resection of DNA breaks. *Cell*. 141:243–254. doi:10.1016/j.cell.2010.03.012

Chen, L., C.J. Nievera, A.Y. Lee, and X. Wu. 2008. Cell cycle-dependent complex formation of BRCA1.CtIP.MRN is important for DNA double-strand break repair. *J. Biol. Chem.* 283:7713–7720. doi:10.1074/jbc.M710245200

Corpet, A., and G. Almouzni. 2009. A histone code for the DNA damage response in mammalian cells? *EMBO J.* 28:1828–1830. doi:10.1038/emboj.2009.180

Cowell, I.G., N.J. Sunter, P.B. Singh, C.A. Austin, B.W. Durkacz, and M.J. Tilby. 2007. gammaH2AX foci form preferentially in euchromatin after ionising-radiation. *PLoS ONE*. 2:e1057. doi:10.1371/journal.pone.0001057

De Koning, L., A. Savignoni, C. Boumendil, H. Rehman, B. Asselain, X. Sastre-Garau, and G. Almouzni. 2009. Heterochromatin protein 1alpha: a hallmark of cell proliferation relevant to clinical oncology. *EMBO Mol Med*. 1:178–191. doi:10.1002/emmm.200900022

Difilippantonio, S., E. Gapud, N. Wong, C.Y. Huang, G. Mahowald, H.T. Chen, M.J. Kruhlak, E. Callen, F. Livak, M.C. Nussenzweig, et al. 2008. 53BP1 facilitates long-range DNA end-joining during V(D)J recombination. *Nature*. 456:529–533. doi:10.1038/nature07476

Dimitrova, N., Y.C. Chen, D.L. Spector, and T. de Lange. 2008. 53BP1 promotes non-homologous end joining of telomeres by increasing chromatin mobility. *Nature*. 456:524–528. doi:10.1038/nature07433

Dinant, C., and M.S. Luijsterburg. 2009. The emerging role of HP1 in the DNA damage response. *Mol. Cell. Biol.* 29:6335–6340. doi:10.1128/MCB.01048-09

Drouet, J., C. Delteil, J. Lefrançois, P. Concannon, B. Salles, and P. Calsou. 2005. DNA-dependent protein kinase and XRCC4-DNA ligase IV mobilization in the cell in response to DNA double strand breaks. *J. Biol. Chem.* 280:7060–7069. doi:10.1074/jbc.M410746200

Essers, J., R.W. Hendriks, S.M. Swagemakers, C. Troelstra, J. de Wit, D. Bootsma, J.H. Hoeijmakers, and R. Kanaar. 1997. Disruption of mouse RAD54 reduces ionizing radiation resistance and homologous recombination. *Cell*. 89:195–204. doi:10.1016/S0092-8674(00)80199-3

FitzGerald, J.E., M. Grenon, and N.F. Lowndes. 2009. 53BP1: function and mechanisms of focal recruitment. *Biochem. Soc. Trans.* 37:897–904. doi:10.1042/BST0370897

Garcia-Higuera, I., T. Taniguchi, S. Ganesan, M.S. Meyn, C. Timmers, J. Hejna, M. Grompe, and A.D. D'Andrea. 2001. Interaction of the Fanconi anemia proteins and BRCA1 in a common pathway. *Mol. Cell*. 7:249–262. doi:10.1016/S1097-2765(01)00173-3

Gérard, A., S.E. Polo, D. Roche, and G. Almouzni. 2006. Methods for studying chromatin assembly coupled to DNA repair. *Methods Enzymol.* 409:358–374. doi:10.1016/S0076-6879(05)09021-X

Goldberg, M., M. Stucki, J. Falck, D. D'Amours, D. Rahman, D. Pappin, J. Bartek, and S.P. Jackson. 2003. MDC1 is required for the intra-S-phase DNA damage checkpoint. *Nature*. 421:952–956. doi:10.1038/nature01445

Goodarzi, A.A., J.C. Jonnalagadda, P. Douglas, D. Young, R. Ye, G.B. Moorhead, S.P. Lees-Miller, and K.K. Khanna. 2004. Autophosphorylation of ataxia-telangiectasia mutated is regulated by protein phosphatase 2A. *EMBO J.* 23:4451–4461. doi:10.1038/sj.emboj.7600455

Goodarzi, A.A., A.T. Noon, D. Deckbar, Y. Ziv, Y. Shiloh, M. Löbrich, and P.A. Jeggo. 2008. ATM signaling facilitates repair of DNA double-strand breaks associated with heterochromatin. *Mol. Cell*. 31:167–177. doi:10.1016/j.molcel.2008.05.017

Green, C.M., and G. Almouzni. 2003. Local action of the chromatin assembly factor CAF-1 at sites of nucleotide excision repair in vivo. *EMBO J.* 22:5163–5174. doi:10.1093/emboj/cdg478

Groth, A., D. Ray-Gallet, J.P. Quivy, J. Lukas, J. Bartek, and G. Almouzni. 2005. Human Asf1 regulates the flow of S phase histones during replicational stress. *Mol. Cell*. 17:301–311. doi:10.1016/j.molcel.2004.12.018

Groth, A., A. Corpet, A.J. Cook, D. Roche, J. Bartek, J. Lukas, and G. Almouzni. 2007a. Regulation of replication fork progression through histone supply and demand. *Science*. 318:1928–1931. doi:10.1126/science.1148992

Groth, A., W. Rocha, A. Verreault, and G. Almouzni. 2007b. Chromatin challenges during DNA replication and repair. *Cell*. 128:721–733. doi:10.1016/j.cell.2007.01.030

Hashiguchi, K., Y. Matsumoto, and A. Yasui. 2007. Recruitment of DNA repair synthesis machinery to sites of DNA damage/repair in living human cells. *Nucleic Acids Res.* 35:2913–2923. doi:10.1093/nar/gkm115

Hoeijmakers, J.H. 2001. DNA repair mechanisms. *Maturitas*. 38:17–22, discussion :22–23. doi:10.1016/S0378-5122(00)00188-2

Holthausen, J.T., C. Wyman, and R. Kanaar. 2010. Regulation of DNA strand exchange in homologous recombination. *DNA Repair (Amst.)*. 9:1264–1272. doi:10.1016/j.dnarep.2010.09.014

Houlard, M., S. Berlivet, A.V. Probst, J.P. Quivy, P. Héry, G. Almouzni, and M. Gérard. 2006. CAF-1 is essential for heterochromatin organization in pluripotent embryonic cells. *PLoS Genet.* 2:e181. doi:10.1371/journal.pgen.0020181

Inoue, A., J. Hyle, M.S. Lechner, and J.M. Lahti. 2008. Perturbation of HP1 localization and chromatin binding ability causes defects in sister-chromatid cohesion. *Mutat. Res.* 657:48–55.

Ishii, S., A. Koshiyama, F.N. Hamada, T.Y. Nara, K. Iwabata, K. Sakaguchi, and S.H. Namekawa. 2008. Interaction between Lim15/Dmc1 and the homologue of the large subunit of CAF-1: a molecular link between recombination and chromatin assembly during meiosis. *FEBS J.* 275:2032–2041. doi:10.1111/j.1742-4658.2008.06357.x

Jackson, S.P., and J. Bartek. 2009. The DNA-damage response in human biology and disease. *Nature*. 461:1071–1078. doi:10.1038/nature08467

Jin, S., and D.T. Weaver. 1997. Double-strand break repair by Ku70 requires heterodimerization with Ku80 and DNA binding functions. *EMBO J.* 16:6874–6885. doi:10.1093/emboj/16.22.6874

Kim, J.A., M. Kruhlak, F. Dotiwala, A. Nussenzweig, and J.E. Haber. 2007. Heterochromatin is refractory to gamma-H2AX modification in yeast and mammals. *J. Cell Biol.* 178:209–218. doi:10.1083/jcb.200612031

Kimura, H., and P.R. Cook. 2001. Kinetics of core histones in living human cells: little exchange of H3 and H4 and some rapid exchange of H2B. *J. Cell Biol.* 153:1341–1353. doi:10.1083/jcb.153.7.1341

Kinner, A., W. Wu, C. Staudt, and G. Iliakis. 2008. Gamma-H2AX in recognition and signaling of DNA double-strand breaks in the context of chromatin. *Nucleic Acids Res.* 36:5678–5694. doi:10.1093/nar/gkn550

Kornberg, R.D., and A. Klug. 1981. The nucleosome. *Sci. Am.* 244:52–64. doi:10.1038/scientificamerican0281-52

Kruhlak, M.J., A. Celeste, G. Dellaire, O. Fernandez-Capetillo, W.G. Müller, J.G. McNally, D.P. Bazett-Jones, and A. Nussenzweig. 2006. Changes in chromatin structure and mobility in living cells at sites of DNA double-strand breaks. *J. Cell Biol.* 172:823–834. doi:10.1083/jcb.200510015

Le Douarin, B., A.L. Nielsen, J.M. Garnier, H. Ichinose, F. Jeanmougin, R. Losson, and P. Chambon. 1996. A possible involvement of TIF1 alpha and TIF1 beta in the epigenetic control of transcription by nuclear receptors. *EMBO J.* 15:6701–6715.

Lewis, L.K., G. Karthikeyan, J. Cassiano, and M.A. Resnick. 2005. Reduction of nucleosome assembly during new DNA synthesis impairs both major pathways of double-strand break repair. *Nucleic Acids Res.* 33:4928–4939. doi:10.1093/nar/gki806

Lisby, M., and R. Rothstein. 2009. Choreography of recombination proteins during the DNA damage response. *DNA Repair (Amst.).* 8:1068–1076. doi:10.1016/j.dnarep.2009.04.007

Lou, Z., C.C. Chini, K. Minter-Dykhouse, and J. Chen. 2003. Mediator of DNA damage checkpoint protein 1 regulates BRCA1 localization and phosphorylation in DNA damage checkpoint control. *J. Biol. Chem.* 278:13599–13602. doi:10.1074/jbc.C300060200

Loyola, A., H. Tagami, T. Bonaldi, D. Roche, J.P. Quivy, A. Imhof, Y. Nakatani, S.Y. Dent, and G. Almouzni. 2009. The HP1alpha-CAF1-SetDB1-containing complex provides H3K9me1 for Suv39-mediated K9me3 in pericentric heterochromatin. *EMBO Rep.* 10:769–775. doi:10.1038/embor.2009.90

Luijsterburg, M.S., C. Dinant, H. Lans, J. Stap, E. Wiernasz, S. Lagerwerf, D.O. Warmerdam, M. Lindh, M.C. Brink, J.W. Dobrucki, et al. 2009. Heterochromatin protein 1 is recruited to various types of DNA damage. *J. Cell Biol.* 185:577–586. doi:10.1083/jcb.200810035

Lukas, C., J. Falck, J. Bartkova, J. Bartek, and J. Lukas. 2003. Distinct spatiotemporal dynamics of mammalian checkpoint regulators induced by DNA damage. *Nat. Cell Biol.* 5:255–260. doi:10.1038/ncb945

Mailand, N., S. Bekker-Jensen, H. Faustrup, F. Melander, J. Bartek, C. Lukas, and J. Lukas. 2007. RNF8 ubiquitylates histones at DNA double-strand breaks and promotes assembly of repair proteins. *Cell*. 131:887–900. doi:10.1016/j.cell.2007.09.040

Maison, C., and G. Almouzni. 2004. HP1 and the dynamics of heterochromatin maintenance. *Nat. Rev. Mol. Cell Biol.* 5:296–304. doi:10.1038/nrm1355

Maison, C., D. Bailly, A.H. Peters, J.P. Quivy, D. Roche, A. Taddei, M. Lachner, T. Jenuwein, and G. Almouzni. 2002. Higher-order structure in pericentric heterochromatin involves a distinct pattern of histone modification and an RNA component. *Nat. Genet.* 30:329–334. doi:10.1038/ng843

Maison, C., D. Bailly, D. Roche, R.M. de Oca, A.V. Probst, I. Vassias, F. Dingli, B. Lombard, D. Loew, J.P. Quivy, and G. Almouzni. 2011. SUMOylation promotes de novo targeting of HP1α to pericentric heterochromatin. *Nat. Genet.* 43:220–227. doi:10.1038/ng.765

Mari, P.O., B.I. Florea, S.P. Persengiev, N.S. Verkaik, H.T. Brüggenwirth, M. Modesti, G. Giglia-Mari, K. Bezstarosti, J.A. Demmers, T.M. Luider, et al. 2006. Dynamic assembly of end-joining complexes requires interaction between Ku70/80 and XRCC4. *Proc. Natl. Acad. Sci. USA*. 103:18597–18602. doi:10.1073/pnas.0609061103

Martini, E., D.M. Roche, K. Marheineke, A. Verreault, and G. Almouzni. 1998. Recruitment of phosphorylated chromatin assembly factor 1 to chromatin after UV irradiation of human cells. *J. Cell Biol.* 143:563–575. doi:10.1083/jcb.143.3.563

McManus, K.J., and M.J. Hendzel. 2005. ATM-dependent DNA damage-independent mitotic phosphorylation of H2AX in normally growing mammalian cells. *Mol. Biol. Cell*. 16:5013–5025. doi:10.1091/mbc.E05-01-0065

Misteli, T., and E. Soutoglou. 2009. The emerging role of nuclear architecture in DNA repair and genome maintenance. *Nat. Rev. Mol. Cell Biol.* 10:243–254. doi:10.1038/nrm2651

Moggs, J.G., P. Grandi, J.P. Quivy, Z.O. Jónsson, U. Hübscher, P.B. Becker, and G. Almouzni. 2000. A CAF-1-PCNA-mediated chromatin assembly pathway triggered by sensing DNA damage. *Mol. Cell. Biol.* 20:1206–1218. doi:10.1128/MCB.20.4.1206-1218.2000

Moné, M.J., M. Volker, O. Nikaido, L.H. Mullenders, A.A. van Zeeland, P.J. Verschure, E.M. Manders, and R. van Driel. 2001. Local UV-induced DNA damage in cell nuclei results in local transcription inhibition. *EMBO Rep.* 2:1013–1017. doi:10.1093/embo-reports/kve224

Mortusewicz, O., and H. Leonhardt. 2007. XRCC1 and PCNA are loading platforms with distinct kinetic properties and different capacities to respond to multiple DNA lesions. *BMC Mol. Biol.* 8:81. doi:10.1186/1471-2199-8-81

Murzina, N., A. Verreault, E. Laue, and B. Stillman. 1999. Heterochromatin dynamics in mouse cells: interaction between chromatin assembly factor 1 and HP1 proteins. *Mol. Cell*. 4:529–540. doi:10.1016/S1097-2765(00)80204-X

Obuse, C., O. Iwasaki, T. Kiyomitsu, G. Goshima, Y. Toyoda, and M. Yanagida. 2004. A conserved Mis12 centromere complex is linked to heterochromatic HP1 and outer kinetochore protein Zwint-1. *Nat. Cell Biol.* 6:1135–1141. doi:10.1038/ncb1187

Peters, A.H., D. O'Carroll, H. Scherthan, K. Mechtler, S. Sauer, C. Schöfer, K. Weipoltshammer, M. Pagani, M. Lachner, A. Kohlmaier, et al. 2001. Loss of the Suv39h histone methyltransferases impairs mammalian heterochromatin and genome stability. *Cell*. 107:323–337. doi:10.1016/S0092-8674(01)00542-6

Pierce, A.J., P. Hu, M. Han, N. Ellis, and M. Jasin. 2001. Ku DNA end-binding protein modulates homologous repair of double-strand breaks in mammalian cells. *Genes Dev.* 15:3237–3242. doi:10.1101/gad.946401

Polo, S.E., and G. Almouzni. 2007. DNA damage leaves its mark on chromatin. *Cell Cycle*. 6:2355–2359. doi:10.4161/cc.6.19.4756

Polo, S.E., D. Roche, and G. Almouzni. 2006. New histone incorporation marks sites of UV repair in human cells. *Cell*. 127:481–493. doi:10.1016/j.cell.2006.08.049

Pommier, Y., C. Redon, V.A. Rao, J.A. Seiler, O. Sordet, H. Takemura, S. Antony, L. Meng, Z. Liao, G. Kohlhagen, et al. 2003. Repair of and checkpoint response to topoisomerase I-mediated DNA damage. *Mutat. Res.* 532:173–203. doi:10.1016/j.mrfmmm.2003.08.016

Quivy, J.P., D. Roche, D. Kirschner, H. Tagami, Y. Nakatani, and G. Almouzni. 2004. A CAF-1 dependent pool of HP1 during heterochromatin duplication. *EMBO J.* 23:3516–3526. doi:10.1038/sj.emboj.7600362

Quivy, J.P., A. Gérard, A.J. Cook, D. Roche, and G. Almouzni. 2008. The HP1-p150/CAF-1 interaction is required for pericentric heterochromatin replication and S-phase progression in mouse cells. *Nat. Struct. Mol. Biol.* 15:972–979. doi:10.1038/nsmb.1470

Rogakou, E.P., D.R. Pilch, A.H. Orr, V.S. Ivanova, and W.M. Bonner. 1998. DNA double-stranded breaks induce histone H2AX phosphorylation on serine 139. *J. Biol. Chem.* 273:5858–5868. doi:10.1074/jbc.273.10.5858

Rogakou, E.P., C. Boon, C. Redon, and W.M. Bonner. 1999. Megabase chromatin domains involved in DNA double-strand breaks in vivo. *J. Cell Biol.* 146:905–916. doi:10.1083/jcb.146.5.905

Rolef Ben-Shahar, T., A.G. Castillo, M.J. Osborne, K.L. Borden, J. Kornblatt, and A. Verreault. 2009. Two fundamentally distinct PCNA interaction peptides contribute to chromatin assembly factor 1 function. *Mol. Cell. Biol.* 29:6353–6365. doi:10.1128/MCB.01051-09

Ryan, R.F., D.C. Schultz, K. Ayyanathan, P.B. Singh, J.R. Friedman, W.J. Fredericks, and F.J. Rauscher III. 1999. KAP-1 corepressor protein interacts and colocalizes with heterochromatic and euchromatic HP1 proteins: a potential role for Krüppel-associated box-zinc finger proteins in heterochromatin-mediated gene silencing. *Mol. Cell. Biol.* 19:4366–4378.

Sartori, A.A., C. Lukas, J. Coates, M. Mistrik, S. Fu, J. Bartek, R. Baer, J. Lukas, and S.P. Jackson. 2007. Human CtIP promotes DNA end resection. *Nature*. 450:509–514. doi:10.1038/nature06337

Schultz, L.B., N.H. Chehab, A. Malikzay, and T.D. Halazonetis. 2000. p53 binding protein 1 (53BP1) is an early participant in the cellular response to DNA double-strand breaks. *J. Cell Biol.* 151:1381–1390. doi:10.1083/jcb.151.7.1381

Scully, R., S. Ganesan, M. Brown, J.A. De Caprio, S.A. Cannistra, J. Feunteun, S. Schnitt, and D.M. Livingston. 1996. Location of BRCA1 in human breast and ovarian cancer cells. *Science*. 272:123–126. doi:10.1126/science.272.5258.123

Shibahara, K., and B. Stillman. 1999. Replication-dependent marking of DNA by PCNA facilitates CAF-1-coupled inheritance of chromatin. *Cell*. 96:575–585. doi:10.1016/S0092-8674(00)80661-3

Song, Y., F. He, G. Xie, X. Guo, Y. Xu, Y. Chen, X. Liang, I. Stagljar, D. Egli, J. Ma, and R. Jiao. 2007. CAF-1 is essential for *Drosophila* development and involved in the maintenance of epigenetic memory. *Dev. Biol.* 311:213–222. doi:10.1016/j.ydbio.2007.08.039

Soria, G., J. Speroni, O.L. Podhajcer, C. Prives, and V. Gottifredi. 2008. p21 differentially regulates DNA replication and DNA-repair-associated processes after UV irradiation. *J. Cell Sci.* 121:3271–3282. doi:10.1242/jcs.027730

Soria, G., L. Belluscio, W.A. van Cappellen, R. Kanaar, J. Essers, and V. Gottifredi. 2009. DNA damage induced Pol eta recruitment takes place independently of the cell cycle phase. *Cell Cycle*. 8:3340–3348. doi:10.4161/cc.8.20.9836

Soutoglou, E., J.F. Dorn, K. Sengupta, M. Jasin, A. Nussenzweig, T. Ried, G. Danuser, and T. Misteli. 2007. Positional stability of single double-strand breaks in mammalian cells. *Nat. Cell Biol.* 9:675–682. doi:10.1038/ncb1591

Stucki, M., J.A. Clapperton, D. Mohammad, M.B. Yaffe, S.J. Smerdon, and S.P. Jackson. 2005. MDC1 directly binds phosphorylated histone H2AX to regulate cellular responses to DNA double-strand breaks. *Cell*. 123:1213–1226. doi:10.1016/j.cell.2005.09.038

Taniguchi, T., I. Garcia-Higuera, P.R. Andreassen, R.C. Gregory, M. Grompe, and A.D. D'Andrea. 2002. S-phase-specific interaction of the Fanconi anemia protein, FANCD2, with BRCA1 and RAD51. *Blood*. 100:2414–2420. doi:10.1182/blood-2002-01-0278

Thiru, A., D. Nietlispach, H.R. Mott, M. Okuwaki, D. Lyon, P.R. Nielsen, M. Hirshberg, A. Verreault, N.V. Murzina, and E.D. Laue. 2004. Structural basis of HP1/PXVXL motif peptide interactions and HP1 localisation to heterochromatin. *EMBO J.* 23:489–499. doi:10.1038/sj.emboj.7600088

van Attikum, H., and S.M. Gasser. 2009. Crosstalk between histone modifications during the DNA damage response. *Trends Cell Biol.* 19:207–217. doi:10.1016/j.tcb.2009.03.001

van Gent, D.C., J.H. Hoeijmakers, and R. Kanaar. 2001. Chromosomal stability and the DNA double-stranded break connection. *Nat. Rev. Genet.* 2:196–206. doi:10.1038/35056049

van Veelen, L.R., J. Essers, M.W. van de Rakt, H. Odijk, A. Pastink, M.Z. Zdzienicka, C.C. Paulusma, and R. Kanaar. 2005. Ionizing radiation-induced foci formation of mammalian Rad51 and Rad54 depends on the Rad51 paralogs, but not on Rad52. *Mutat. Res.* 574:34–49. doi:10.1016/j.mrfmmm.2005.01.020

Wang, H., L. Wang, H. Erdjument-Bromage, M. Vidal, P. Tempst, R.S. Jones, and Y. Zhang. 2004. Role of histone H2A ubiquitination in Polycomb silencing. *Nature*. 431:873–878. doi:10.1038/nature02985

Wyman, C., and R. Kanaar. 2006. DNA double-strand break repair: all's well that ends well. *Annu. Rev. Genet.* 40:363–383. doi:10.1146/annurev.genet.40.110405.090451

Xie, A., A. Hartlerode, M. Stucki, S. Odate, N. Puget, A. Kwok, G. Nagaraju, C. Yan, F.W. Alt, J. Chen, et al. 2007. Distinct roles of chromatin-associated proteins MDC1 and 53BP1 in mammalian double-strand break repair. *Mol. Cell*. 28:1045–1057. doi:10.1016/j.molcel.2007.12.005

Yu, X., and J. Chen. 2004. DNA damage-induced cell cycle checkpoint control requires CtIP, a phosphorylation-dependent binding partner of BRCA1 C-terminal domains. *Mol. Cell. Biol.* 24:9478–9486. doi:10.1128/MCB.24.21.9478-9486.2004

Yu, X., L.C. Wu, A.M. Bowcock, A. Aronheim, and R. Baer. 1998. The C-terminal (BRCT) domains of BRCA1 interact in vivo with CtIP, a protein implicated in the CtBP pathway of transcriptional repression. *J. Biol. Chem.* 273:25388–25392. doi:10.1074/jbc.273.39.25388

Zarebski, M., E. Wiernasz, and J.W. Dobrucki. 2009. Recruitment of heterochromatin protein 1 to DNA repair sites. *Cytometry A*. 75:619–625.

Ziv, Y., D. Bielopolski, Y. Galanty, C. Lukas, Y. Taya, D.C. Schultz, J. Lukas, S. Bekker-Jensen, J. Bartek, and Y. Shiloh. 2006. Chromatin relaxation in response to DNA double-strand breaks is modulated by a novel ATM- and KAP-1 dependent pathway. *Nat. Cell Biol.* 8:870–876. doi:10.1038/ncb1446